Electronic Supplementary Material (ESI) for New Journal of Chemistry.

Synthesis and structural characterisation of bulky heptaaromatic (hetero)-aryl *o*-substituted *s*-aryltetrazines

Clève D. Mboyi, Ahmad Daher, Neelab Khirzada, Charles H. Devillers, Hélène Cattey, Paul Fleurat-Lessard, Julien Roger and Jean-Cyrille Hierso

Table of contents

General conditions

All reagents were purchased from commercial suppliers and used without purifications. Reactions were performed in Schlenk tubes or in a microwave reaction vessel. The microwave reactions were run in closed reaction vessels with magnetic stirring and with the temperature controlled via IR detection. NMR spectra were recorded on Bruker spectrometers: Bruker Avance III 300 spectrometer (^{1}H 300.13 MHz, ^{19}F 282.40 MHz; ^{13}C 75.47 MHz) or Avance Neo 500 MHz (^{1}H 500 MHz, ^{19}F 470 MHz, ^{13}C 125 MHz) equipped with a 5 mm BBOF iProbe. NMR spectroscopy chemical shifts are quoted in parts per million (δ) relative to TMS (for ^{1}H, ^{13}C) and $CFCl_3$ (for ^{19}F). For ^{1}H and ^{13}C spectra, calibration was made by using residual signals of partially deuterated solvent. Flash chromatography was performed on silica gel (230-400 mesh). High-resolution mass spectrometry (HRMS) analyses were recorded on a LTQ XL Orbitrap (Thermo Scientific) equipped with an electrospray ionization source (HESI 2). UV-visible absorption spectra in solution were recorded with a Varian UV-vis spectrophotometer Cary 50 scan using quartz cells (Hellma).

General procedure for *o*-tetrabromination of 1 under microwave conditions

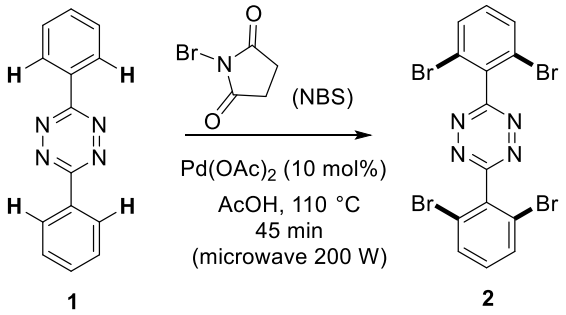

***Scheme S-1*.** *B*romination reactions on 3,6-diphenyl-1,2,4,5-tetrazine **1** for brominated tetrazine **2**.

In a microwave reaction vessel equipped with a magnetic stirring bar, 3,6-diphenyl-1,2,4,5-tetrazine **(1)** (1 equiv, 0.855 mmol, 0.20 g), [$Pd(OAc)_2$] (20 mol%), NBS (8 equiv, 1.22 g) and acetic acid (0.125 M) were introduced, the vessel was placed in a microwave reactor (120 °C, 200 W, 45 min). After cooling down to room temperature, the reaction mixture was extracted with distilled water and dichloromethane, the combined organic layers were dried over anhydrous $MgSO_4$, filtrated and the solvent was evaporated under reduced pressure. The crude product was purified by silica gel column chromatography to afford **2** as purple solid. R_f = 0.50 (ethyl acetate/heptane = 2:8 (v/v)). Yield = 89%. ^{1}H NMR (500 MHz, $CDCl_3$), δ = 7.77 (d, *J* = 8.1 Hz, 4H), 7.41-7.33 (m, 2H). The analyses were identical to reported data (*Angew. Chem. Int. Ed. 2016, 55, 5555 –5559*).

Synthesis of heptaaromatic *o*-substituted *s*-aryltetrazines 3-13

In a dried Schlenk tube equipped with magnetic stirring bar were added the 3,6-bis(2,6-dibromophenyl)-1,2,4,5-tetrazine **2** (1 equiv), (hetero)arylboronic acid (8 equiv), $[Pd_2(dba)_3]$ (20 mol%), K_2CO_3 (8 equiv). Dry toluene (typically 0.023 M) was added, and the Schlenk tube was purged three times with argon. The Schlenk tube was placed in a pre-heated oil bath at 110 °C for 16 h. After cooling down to room temperature, the reaction mixture was extracted with distilled water and dichloromethane, the combined organic layers were dried over anhydrous $MgSO_4$, filtrated, and the solvent was evaporated under reduced pressure. The products **3-13** were purified by silica gel column chromatography (eluent: heptane/dichloromethane or ethyl acetate). Crystallization for single crystal was typically achieved from volatile $CHCl_3$ or $CH2Cl_2$ solvent (see ESI for XRD).

3,6-di([1,1':3',1''-terphenyl]-2'-yl)-1,2,4,5-tetrazine (3)

(2) (1 equiv, 0.273 mmol, 0.150 g), $[Pd_2(dba)_3]$ (20 mol%), phenylboronic acid (8 equiv, 2.183 mmol, 0.266 g), K_2CO_3 (8 equiv, 2.183 mmol, 0.302 g), toluene (0.023 M), 110 °C, 16 h.

R_f = 0.46 (ethyl acetate/heptane = 2:8 (v/v)). Yield = 95%.

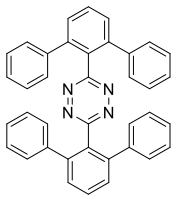

^{1}H NMR (300 MHz, $CDCl_3$): δ (ppm) = 7.62 (dd, *J* = 8.4, 7.0 Hz, 2H), 7.48 (dd, *J* = 7.7, 0.7 Hz, 4H), 7.24-7.18 (m, 12H), 7.02-6.94 (m, 8H).

^{13}C NMR (75 MHz, $CDCl_3$): δ (ppm) = 166.4, 143.1, 140.2, 130.9, 130.4, 130.1, 129.6, 128.1, 127.1.

Elemental analysis: Calcd (%) for $C_{38}H_{26}N_4 \cdot 1.5H_2O \cdot 0.5$ toluene: C: 81.48, H: 5.44, N: 9.16. Found: C:81.83, H: 5.68, N: 9.21.

HRMS + p ESI (m/z) [M+H$^+$] Calcd for $C_{38}H_{26}N_4$: 539.2230. Found: m/z = 539.2254.

3,6-bis(4,4''-di-tert-butyl-[1,1':3',1''-terphenyl]-2'-yl)-1,2,4,5-tetrazine (4)

(2) (1 equiv, 0.0455 mmol, 0.025 g), $[Pd_2(dba)_3]$ (20 mol%), (4-(*tert*-butyl)phenyl)boronic acid (8 equiv, 0.364 mmol, 0.064 g), K_2CO_3 (8 equiv, 0.364 mmol, 0.050 g), toluene (0.023 M), 110 °C, 16 h.

R_f = 0.42 (Ethyl acetate/heptane = 2:8 (v/v)). Yield = 69%.

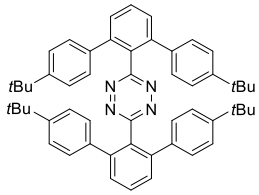

^{1}H NMR (500 MHz, $CDCl_3$): δ (ppm) = 7.59 (dd, *J* = 8.2, 7.2 Hz, 2H), 7.46 (d, *J* = 7.7 Hz, 4H), 7.29 (d, *J* = 8.7 Hz, 8H), 6.91 (d, *J* = 7.9 Hz, 8H), 1.30 (s, 36H).

^{13}C NMR (75 MHz, $CDCl_3$): δ (ppm) = 166.4, 149.9, 142.9, 137.3, 130.8, 130.3, 130.1, 129.3, 125.1, 34.5, 31.4.

Elemental analysis: Calcd (%) for $C_{54}H_{58}N_4 \cdot 0.5H_2O \cdot 0.5$ heptane: C: 84.0, H: 8.21, N: 6.81. Found: C:84.1, H: 8.39, N: 6.88.

HRMS + p ESI (m/z) [M+H$^+$] Calcd for C_{54} H_{58} N_4: 763,4734. Found: m/z = 763,4759.

3,6-bis(4,4''-dimethoxy-[1,1':3',1''-terphenyl]-2'-yl)-1,2,4,5-tetrazine (5)

(2) (1 equiv, 0.0455 mmol, 0.025 g), $[Pd_2(dba)_3]$ (20 mol%), (4-methoxyphenyl)boronic acid (8 equiv, 0.364 mmol, 0.055 g), K_2CO_3 (8 equiv, 0.364 mmol, 0.050 g), toluene (0.023 M), 110 °C, 16 h.

R_f = 0.16 (ethyl acetate/heptane = 2:8 (v/v)). Yield = 80%.

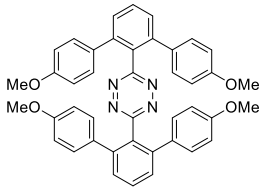

Rf = 0.32 (dichloromethane/heptane = 1/1 (v/v)).

^{1}H NMR (300 MHz, $CDCl_3$): δ (ppm) = 7.58 (dd, *J* = 8.1, 7.3 Hz, 2H), 7.44 (d, *J* = 7.7 Hz, 4H), 6.94-6.88 (m, 8H), 6.75-6.69 (m, 8H), 3.76 (s, 12H).

^{13}C NMR (75 MHz, $CDCl_3$): δ (ppm) = 166.6, 158.7, 142.7, 132.6, 131.0, 130.8, 130.4, 129.8, 113.6, 55.2.

Elemental analysis: Calcd (%) for $C_{42}H_{34}N_4O_4 \cdot 1.5H_2O \cdot 0.6$toluene$\cdot 1CH_2Cl_2$: C: 68.63, H: 5.34, N: 6.78. Found: C:68.91, H: 5.72, N: 6.79.

HRMS + p ESI (m/z) [M+H$^+$] Calcd for $C_{42}H_{34}N_4O_4$: 659,2652. Found: m/z = 659,2655.

3,6-bis(4,4''-difluoro-[1,1':3',1''-terphenyl]-2'-yl)-1,2,4,5-tetrazine (6)

(2) (1 equiv, 0.0455 mmol, 0.025 g), $[Pd_2(dba)_3]$ (20 mol%), (4-fluorophenyl)boronic acid (8 equiv, 0.364 mmol, 0.051 g), K_2CO_3 (8 equiv, 0.364 mmol, 0.050 g), toluene (0.023 M), 110 °C, 16 h.

R_f = 0.46 (ethyl acetate/heptane = 2:8 (v/v)). Yield = 93%.

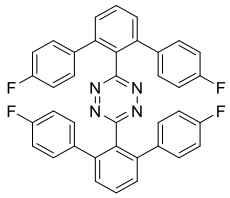

^{1}H NMR (300 MHz, $CDCl_3$): δ (ppm) = 7.61 (dd, *J* = 8.3, 7.2 Hz, 2H), 7.46-7.38 (m, 4H), 7.03-6.92 (m, 8H), 6.89-6.78 (m, 8H).

^{19}F NMR (470 MHz, $CDCl_3$): δ (ppm) = -114.5.

^{13}C NMR (75 MHz, $CDCl_3$): δ (ppm) = 165.3, 162.5 (d, *J* = 247.0 Hz), 141.0, 134.8, 134.7, 130.2 (d, *J* = 8.2 Hz), 129.3, 128.9, 114.0 (d, *J* = 21.7 Hz).

Elemental analysis: Calcd (%) for $C_{38}H_{22}F_4N_4 \cdot 0.6H_2O \cdot 0.4$ heptane: C: 74.08, H: 4.51, N: 8.47. Found: C:73.68, H: 4.83, N: 8.87.

HRMS + p ESI (m/z) [M+H$^+$] Calcd for $C_{38}H_{23}F_4N_4$: 611.1853. Found: 611.1853.

3,6-bis(4,4''-dibromo-[1,1':3',1''-terphenyl]-2'-yl)-1,2,4,5-tetrazine (7)

(2) (1 equiv, 0.109 mmol, 0.060 g), $[Pd_2(dba)_3]$ (20 mol%), (4-bromophenyl)boronic acid (8 equiv, 0.879 mmol, 0.177 g), K_2CO_3 (8 equiv, 0.879 mmol, 0.121 g), toluene (0.04 M), 110 °C, 16 h.

R_f = 0.52 (Ethyl acetate/heptane = 2:8 (v/v)). Yield = 55%.

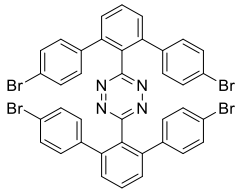

^{1}H NMR (500 MHz, $CDCl_3$): δ (ppm) = 7.63 (t, *J* = 7.7 Hz, 2H), 7.43 (d, *J* = 7.7 Hz, 4H), 7.34-7.28 (m, 8H), 6.92-6.86 (m, 8H).

^{13}C NMR (125 MHz, $CDCl_3$): δ (ppm) = 166.6, 142.4, 138.9, 131.6, 131.5, 131.1, 130.9, 130.3, 122.1.

Elemental analysis: Calcd (%) for $C_{38}H_{22}Br_4N_4 \cdot H_2O$: C: 52.33, H: 2.77, N: 6.42. Found: C:52.56, H: 2.77, N: 6.23.

HRMS + p ESI (m/z) [M+H$^+$] Calcd for $C_{38}H_{23}Br_4N_4$: 850.8650. Found: 850.8663.

3,6-bis(4,4''-trifluoromethyl-[1,1':3',1''-terphenyl]-2'-yl)-1,2,4,5-tetrazine (8)

(2) (1 equiv, 0.046 mmol, 0.025 g), $[Pd_2(dba)_3]$ (20 mol%), (4-trifluoromethyl)phenylboronic acid (8 equiv, 0.879 mmol, 0.069 g), K_2CO_3 (8 equiv, 0.368 mmol, 0.05 g), toluene (0.023 M), 130 °C, 16 h.

R_f = 0.48 (ethyl acetate/heptane = 2:8 (v/v)). Yield = 84%.

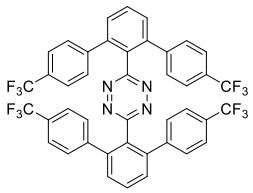

^{1}H NMR (500 MHz, $CDCl_3$): δ (ppm) = 7.71-7.66 (m, 2H), 7.48 (d, *J* = 7.7 Hz, 4H), 7.43-7.37 (m, 8H), 7.12 (d, *J* = 7.9 Hz, 8H).

^{19}F NMR (470 MHz, $CDCl_3$): δ (ppm) = - 62.6.

^{13}C NMR (125 MHz, $CDCl_3$): δ (ppm) = 164.9, 142.3, 140.8, 129.7, 129.6, 129.3, 128.9, 128.7 (q, *J* = 32.7 Hz), 126.1 (q, *J* = 4.0 Hz), 124.0 (q, *J* = 272.1 Hz).

Elemental analysis: Calcd (%) for $C_{42}H_{22}F_{12}N_4 \cdot 2H_2O \cdot 0.2$ heptane: C: 60.14, H: 3.4, N: 6.46. Found: C:60.01, H: 3.65, N: 6.41.

HRMS + p ESI (m/z) [M+H$^+$] Calcd for $C_{42}H_{23}F_{12}N_4$: 811.1725. Found: m/z = 811.1752.

3,6-bis(4,4''-acetyl-[1,1':3',1''-terphenyl]-2'-yl)-1,2,4,5-tetrazine (9)

(2) (1 equiv, 0.046 mmol, 0.025 g), $[Pd_2(dba)_3]$ (20 mol%), (4-acethyl)phenylboronic acid (8 equiv, 0.879 mmol, 0.06 g), K_2CO_3 (8 equiv, 0.368 mmol, 0.05 g), toluene (0.023 M), 130 °C, 16 h.

R_f = 0.10 (ethyl acetate/heptane = 4:6 (v/v)). Yield = 37%.

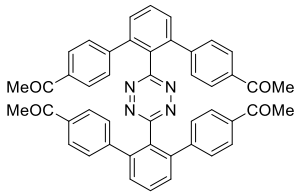

^{1}H NMR (500 MHz, $CDCl_3$): δ (ppm) = 7.80 (d, *J* = 8.5 Hz, 8H), 7.68 (t, *J* = 7.8 Hz, 2H), 7.50 (d, *J* = 7.7 Hz, 4H), 7.06 (d, *J* = 8.4 Hz, 8H), 2.63 (s, 12H).

^{13}C NMR (125 MHz, $CDCl_3$): δ (ppm) = 197.5, 166.1, 144.6, 142.2, 135.9 130.8, 130.5, 130.3, 129.8, 128.2, 26.7.

Elemental analysis: Calcd (%) for $C_{46}H_{34}N_4O_4 \cdot 0.5H_2O \cdot 0.55\ CH_2Cl_2 \cdot 0.15\ C_{38}H_{27}N_4O_3Br$: C: 72.75, H: 4.69, N: 7.47. Found: C:72.65, H: 4.96, N: 7.86., where $C_{38}H_{27}N_4O_3Br$ is the 3-((4'-acetyl)-3-bromo-[1,1'-biphenyl]-2'-yl))-6-(4,4''-acetyl-[1,1':3',1''-terphenyl]-2'-yl)-1,2,4,5-tetrazine.

HRMS + p ESI (m/z) [M+H$^+$] Calcd for $C_{46}H_{35}N_4O_4$: 708.2731. Found: m/z = 708.2686.

3,6-bis(3,3''-dimethoxy-[1,1':3',1''-terphenyl]-2'-yl)-1,2,4,5-tetrazine (10)

(2) (1 equiv, 0.0455 mmol, 0.025 g), $[Pd_2(dba)_3]$ (20 mol%), (3-methoxyphenyl)boronic acid (8 equiv, 0.364 mmol, 0.055 g), K_2CO_3 (8 equiv, 0.364 mmol, 0.050 g), toluene (0.023 M), 110 °C, 16 h.

R_f = 0.22 (ethyl acetate/heptane = 2:8 (v/v)). Yield = 66%.

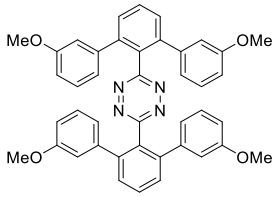

^{1}H NMR (500 MHz, $CDCl_3$) δ (ppm) = 7.61 (dd, *J* = 8.2, 7.2 Hz, 2H), 7.48 (d, *J* = 7.6 Hz, 4H), 7.06 (t, *J* = 8.0 Hz, 4H), 6.84 (dd, *J* = 2.6, 1.6 Hz, 4H), 6.73 (ddd, *J* = 8.4, 2.5, 0.9 Hz, 4H), 6.29 (dt, *J* = 7.8, 1.1 Hz, 4H), 3.75 (s, 12H).

^{13}C NMR (125 MHz, $CDCl_3$): δ (ppm) = 166.4, 159.5, 143.1, 141.5, 130.8, 130.3, 130.1, 128.9, 122.2, 115.4, 112.6, 55.1.

Elemental analysis: Calcd (%) for $C_{42}H_{34}N_4O_4 \cdot 0.3CH_2Cl_2 \cdot 1.4$toluene: C: 76.95, H: 5.68, N: 6.89. Found: C:76.87, H: 5.28, N: 6.54.

HRMS + p ESI (m/z) $[M+H^+]$ Calcd for $C_{42}H_{35}N_4O_4$: 659.2652. Found: m/z = 659.2660.

3,6-bis(3,3''-dibromo-[1,1':3',1''-terphenyl]-2'-yl)-1,2,4,5-tetrazine (11)

(2) (1 equiv, 0.109 mmol, 0.060 g), $[Pd_2(dba)_3]$ (20 mol%), (4-bromophenyl)boronic acid (8 equiv, 0.879 mmol, 0.177 g), K_2CO_3 (8 equiv, 0.879 mmol, 0.121 g), toluene (0.04 M), 110 °C, 16 h.

R_f = 0.52 (ethyl acetate/heptane = 2:8 (v/v)). Yield = 58%.

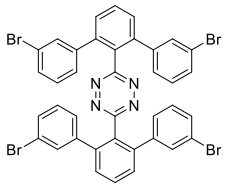

^{1}H NMR (500 MHz, $CDCl_3$): δ (ppm) = 7.67-7.60 (t, *J* = 10.0 Hz, 2H), 7.49 (t, *J* = 1.8 Hz, 4H), 7.45 (d, *J* = 7.7 Hz, 4H), 7.36 (m, 4H), 6.91 (t, *J* = 7.9 Hz, 4H), 6.66-6.60 (m, 4H).

^{13}C NMR (125 MHz, $CDCl_3$): δ (ppm) = 166.3, 142.2, 142.1, 132.9, 130.9, 130.9, 130.9, 130.8, 129.6, 128.4, 122.9, 77.6.

Elemental analysis: Calcd (%) for $C_{38}H_{22}Br_4N_4 \cdot 0.3CH_2Cl_2$: C: 49.88, H: 2.58, N: 5.97. Found: C:50.21, H: 2.38, N: 5.98.

HRMS + p ESI (m/z) $[M+H^+]$ Calcd for $C_{38}H_{23}Br_4N_4$: 850.8650. Found: m/z 850=8659.

3,6-bis(2,6-di(thiophen-2-yl)phenyl)-1,2,4,5-tetrazine (12)

(2) (1 equiv, 0.183 mmol, 0.100 g), $[Pd_2(dba)_3]$ (20 mol%), thiophen-3-ylboronic acid (8 equiv, 1.464 mmol, 0.187 g), K_2CO_3 (8 equiv, 1.464 mmol, 0.202 g), toluene (0.046 M), 130 °C, 16 h.

Rf = 0.4 (ethyl acetate/heptane = 2:8 (v/v)). Yield = 13%.

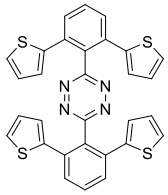

^{1}H NMR (500 MHz, $CDCl_3$): δ (ppm) = 7.61 (d, *J* = 3.2 Hz, 6H), 7.19 (dd, *J* = 5.2, 1.2 Hz, 4H), 6.83 (dd, *J* = 5.2, 3.5 Hz, 4H), 6.57 (dd, *J* = 3.5, 1.2 Hz, 4H).

^{13}C NMR (125 MHz, $CDCl_3$): δ (ppm) = 165.8, 139.8, 134.74, 131.3, 129.7, 129.3, 127.3, 126.1, 125.6.

Elemental analysis: Calcd (%) for $C_{30}H_{18}N_4S_4 \cdot 2H_2O$: C: 60.18, H: 3.7, N: 9.36. Found: C:60.54, H: 3.68, N: 9.34.

HRMS + p ESI (m/z) $[M+Na^+]$ Calcd for $C_{30}H_{18}N_4S_4Na$: 585.0306. Found: m/z = 585.0303.

3,6-bis(2,6-di(thiophen-3-yl)phenyl)-1,2,4,5-tetrazine (13)

(2) (1 equiv, 0.183 mmol, 0.100 g), $[Pd_2(dba)_3]$ (20 mol%), thiophen-3-ylboronic acid (8 equiv, 1.464 mmol, 0.187 g), K_2CO_3 (8 equiv, 1.464 mmol, 0.202 g), toluene (0.046 M), 130 °C, 16 h.

Rf = 0.4 (ethyl acetate/heptane = 2:8 (v/v)). Yield = 47%.

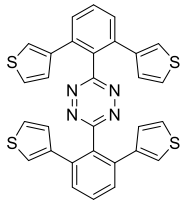

^{1}H NMR (500 MHz, $CDCl_3$): δ (ppm) = 7.60 (dd, *J* = 8.4, 7.0 Hz, 2H), 7.54-7.50 (m, 4H), 7.19 (dd, *J* = 5.0, 3.0 Hz, 4H), 6.79 (dd, *J* = 5.0, 1.3 Hz, 4H), 6.76 (dd, *J* = 3.0, 1.3 Hz, 4H).

^{13}C NMR (125 MHz, $CDCl_3$): δ (ppm) = 167.2, 140.3, 137.8, 131.6, 130.4, 129.4, 129.0, 125.7, 124.4.

Elemental analysis: Calcd (%) for $C_{30}H_{18}N_4S_4 \cdot 1.6H_2O$: C: 60.91, H: 3.61, N: 9.47. Found: C:60.68, H: 3.72, N: 9.47.

HRMS + p ESI (m/z) [$M+H^+$] Calcd for $C_{30}H_{19}N_4S_4$: 563.0487. Found: m/z = 563.0482.

UV-Vis measurements

The absorption spectra of **2-13** in dichloromethane are displayed in Figure S-1 (Figure S-2: zoom between 235–430 nm; Figure S-3: zoom between 430–650 nm) and the absorption data are given in Table S-1. The absorption spectra to visualize the maximum absorption bands were recorded at $8.0x10^{-5}$-$9.0x10^{-5}$ M.

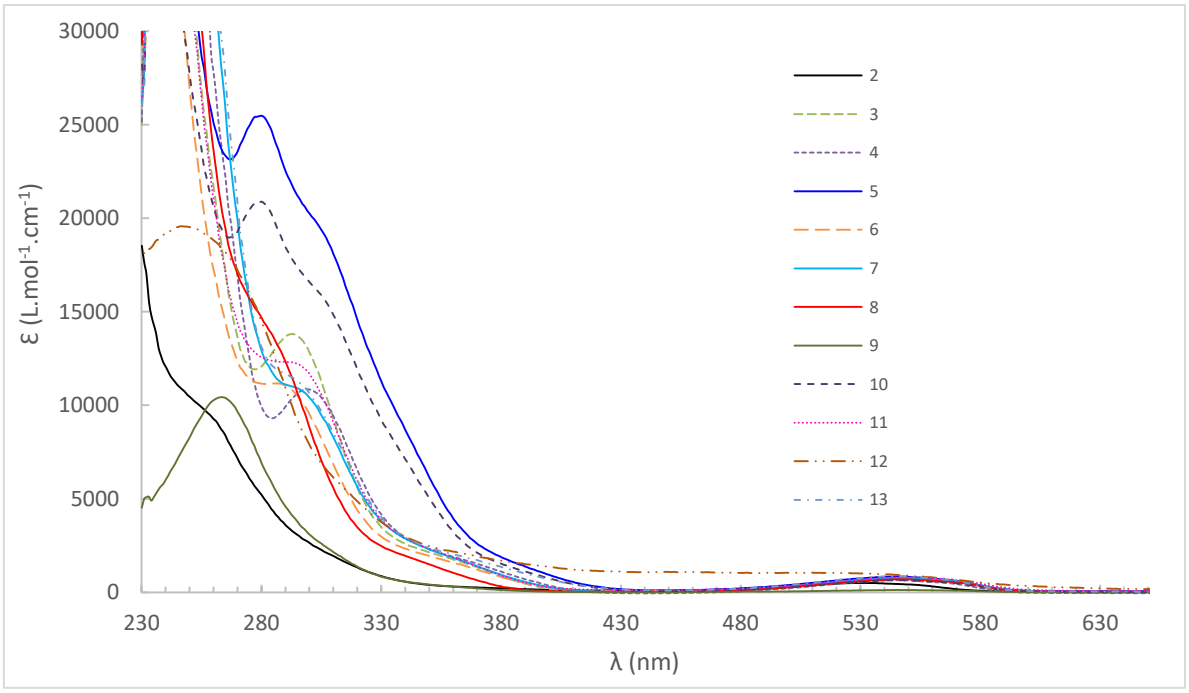

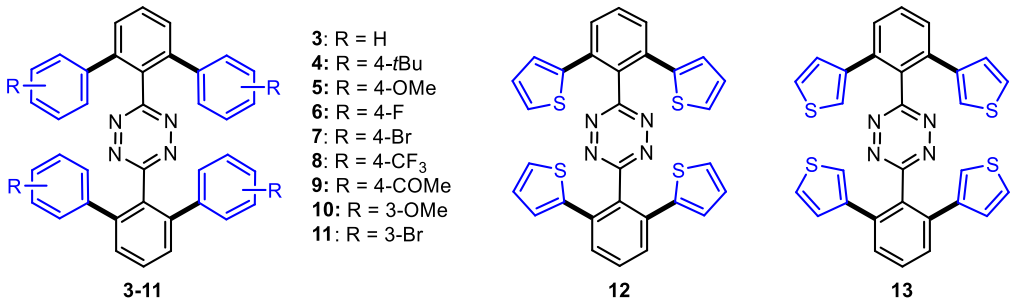

***Figure S-1*:** Molar absorption coefficient of compounds of tetrazines **2-13** in dichloromethane at $8.0\text{-}9.0.10^{-5}$ M.

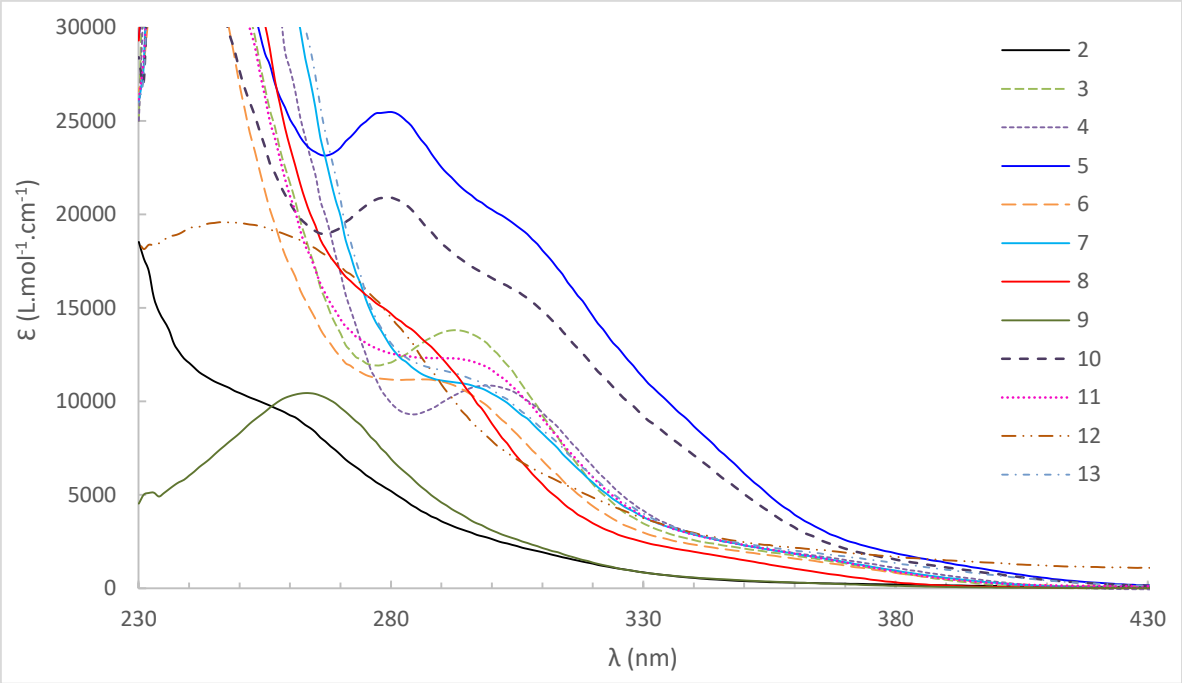

***Figure S-2*: Molar absorption coefficient of compounds of tetrazines **2-13** in dichloromethane at 8.0-9.0.10^{-5} M (zooming 235–430 nm).**

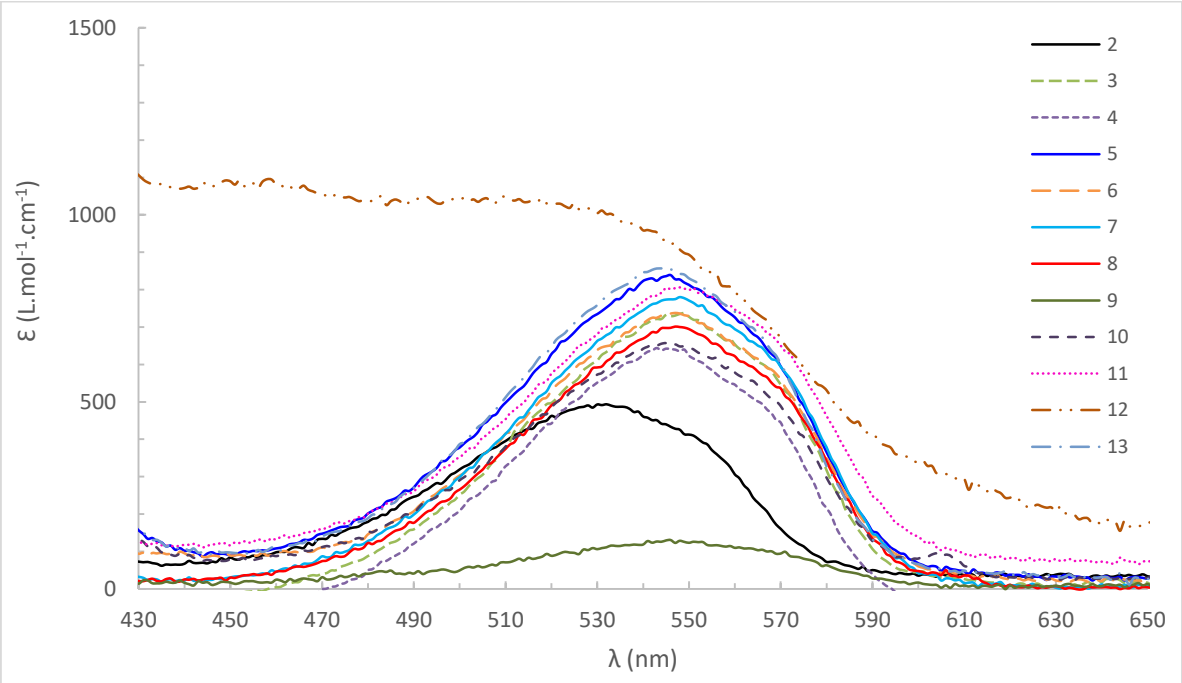

***Figure S-3*: Molar absorption coefficient of compounds of tetrazines **2-13** in dichloromethane at about 8.0-9.0.10^{-5} M (zooming 430–650 nm).**

***Table S-1*:** Photophysical properties for compounds **2-13** in dichloromethane: Absorption wavelength (λ, nm) molar absorption coefficient (Ɛ, $L.mol^{-1}.cm^{-1}$).[a]

Tz	**λ_1 (nm)**	**ε_1 (λ_1) ($L.mol^{-1}.cm^{-1}$)**	**λ_2 (nm)**	**ε_2 (λ_2) ($L.mol^{-1}.cm^{-1}$)**
2	260	9 253	532	515
3	296	13 910	550	700
4	302	11 069	548	696
5	282	25 120	548	771
6	284	11 458	549	732
7	294	11 285	549	796
8	284	14 270	549	652
9	265	10 456	550	594
10	281	21 369	548	652
11	295	12 577	550	752
12	243	19 330	522	933
13	291	11 845	547	807

[a] λ_{max} at the maximum of absorbance and the molar extinction coefficients are determined from solutions prepared at a concentration ranging from 10^{-3} to 10^{-5} M in CH_2Cl_2 at room temperature with one cm optical path in quartz cell.

Cyclic voltammetry measurements

All manipulations were performed using Schlenk techniques in an oxygen-free atmosphere of dry argon at room temperature (T = 20 °C ± 3 °C). The supporting electrolyte, tetra-*n*-butylammonium hexafluorophosphate ($TBAPF_6$), was degassed under vacuum before use and then dissolved in CH_2Cl_2 to a concentration of 0.1 mol L^{-1}. Voltammetric analyses were carried out in a standard three-electrode cell with an Autolab PGSTAT 302 N potentiostat, connected to an interfaced computer that employed Electrochemistry Nova software (v. 1.11). The reference electrode was a KCl saturated calomel electrode (SCE) separated from the analyzed solution by a sintered glass disk filled with the background solution. The auxiliary electrode was a platinum foil separated from the analyzed solution by a sintered glass disk filled with the background solution. For all voltammetric measurements, the working electrode was a glassy carbon (GC) electrode (Ø = 3 mm). Before each voltammetric analysis, the GC electrode was polished with a diamond suspension. In these conditions, when operating in CH_2Cl_2 (0.1 M $TBAPF_6$), the formal potential for the ferrocene (+/0) couple was +0.46 V *vs.* SCE.

Figure S-4 and **Table S-2**: Comparison of the substrates 3,6-bis(phenyl)-1,2,4,5-tetrazine **1** and 3,6-bis (2,6-dibromophenyl)-1,2,4,5-tetrazine **2** as well as the heptaaromatic tetrazine **3** (unsubstituted), **4** (bearing a donor group *t*Bu) and **8** (bearing a withdrawing group CF_3).

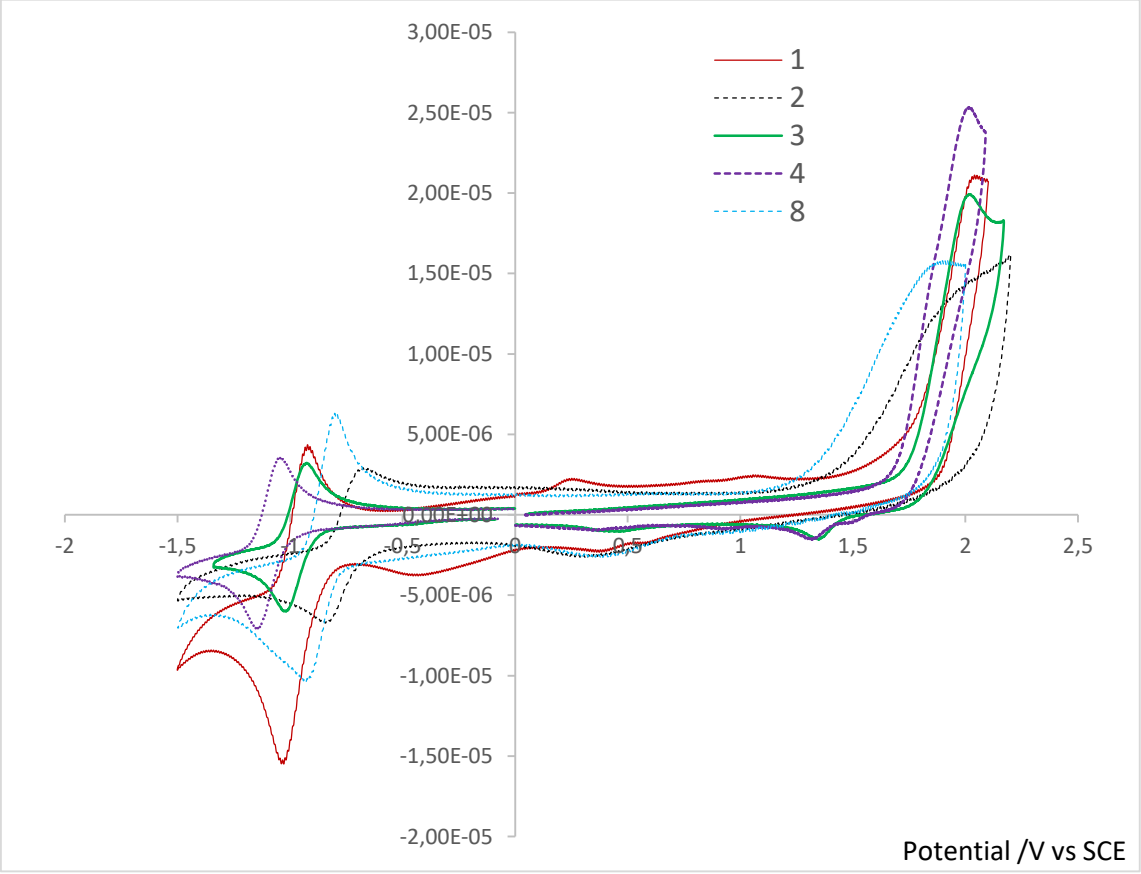

Figure S-4: Cyclic voltammograms of **1-4**, **8** in CH_2Cl_2 0.1 M $TBAPF_6$. Concentration: 10^{-3} M; WE: glassy carbon Ø = 3 mm, v = 100 mV s^{-1}.

Table S-2: Redox events in **1-4** and **8**.

		Red				Ox
Entry	**Compound**	E_{pa} **(V)**	E_{pc} **(V)**	$E_{1/2}$**(V)**	ΔE_p **(mV)**	E_{pa} **(V)**
1	**1**	-0.92	-1.04	-0.98	120	2.05
2	**2**	-0.69	-0.82	-0.76	130	2.07
3	**3**	-0.925	-1.02	-0.98	95	2.02
4	**4**	-1.04	-1.14	-1.09	105	2.02
5	**8**	-0.79	-0.96	-0.88	170	1.88

Figure S-5 and **Table S-3**: Effect of donor substituents OMe in the *para* position (compound **5**) and the *meta* position (compound **10**).

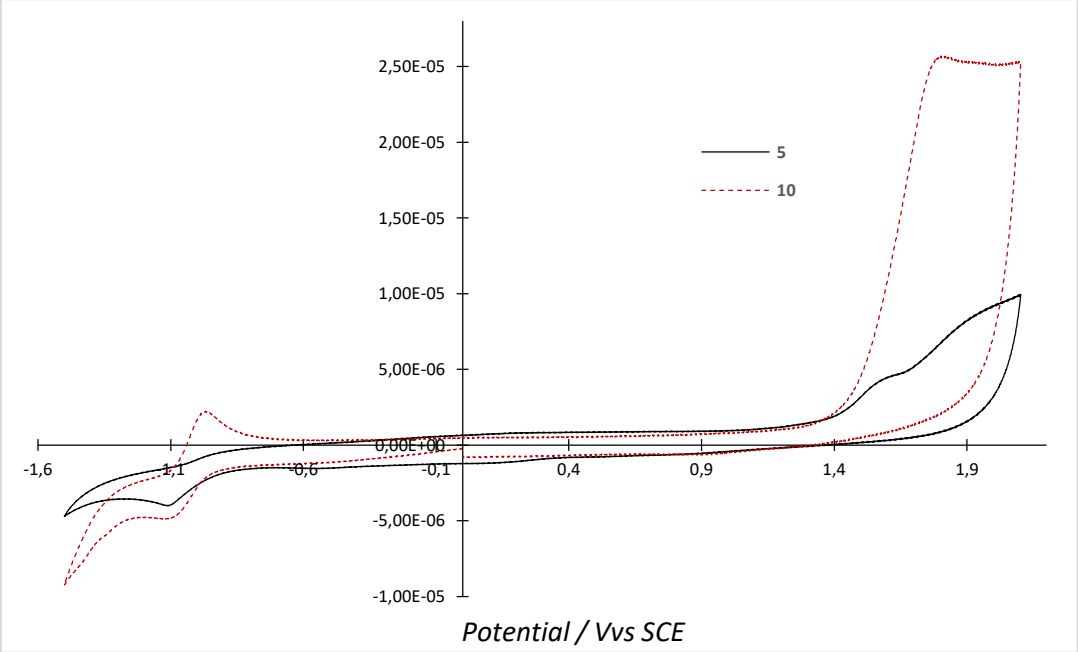

Figure S-5: Cyclic voltammograms of **5** (solid black line) and **10** (red dashed line) in CH_2Cl_2 0.1 M $TBAPF_6$. Concentration: 10^{-3} M; WE: glassy carbon Ø = 3 mm, ν = 100 mV s^{-1}.

Table S-3: Redox events in **5** and **10**.

		Red				Ox
Entry	**Compound**	E_{pa} **(V)**	E_{pc} **(V)**	$E_{1/2}$**(V)**	ΔE_p **(mV)**	E_{pa} **(V)**
1	**5**	-0.91	-1.08	-0.99	170	1.81
2	**10**	-0.97	-1.09	-1.03	120	1.59

Figure S-6 and **Table S-4**: Effect of withdrawing –Br substituents in the *para* position (compound **7**) and in the *meta* position (compound **11**).

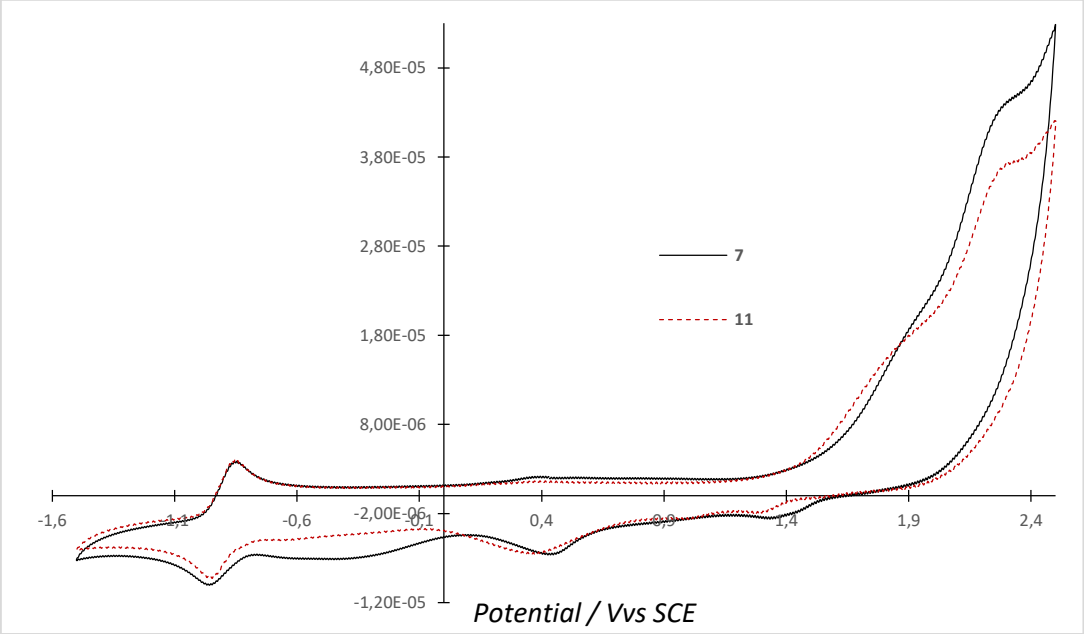

Figure S-6: Cyclic voltammograms of **7** (solid black line) and **11** (red dashed line) in CH_2Cl_2 0.1 M $TBAPF_6$. Concentration: 10^{-3} M; WE: glassy carbon Ø = 3 mm, v = 100 mV s^{-1}.

Table S-4: Redox events in **7** and **11**.

		Red				**Ox**	
Entry	**Compound**	E_{pa} **(V)**	E_{pc} **(V)**	$E_{1/2}$**(V)**	ΔE_p **(mV)**	E_{pa} **(O_1) (V)**	E_{pa} **(O_2) (V)**
1	**7**	-0.83	-0.95	-0.89	120	≈1.87	2.29
2	**11**	-0.83	-0.95	-0.89	120	≈1.87	2.29

Computational Study

Computational details

Quantum mechanics calculations were performed with the Gaussian16 software package.[1] Energy and forces were computed by density functional theory with the hybrid M06-2X exchange-correlation functional.[2] Geometries were optimized and characterized with the aug-cc-pVTZ basis set.[3] Geometries are shown using CylView.[4] The non-covalent interactions were visualized with the Independent Gradient Model[5] that can be seen as an extension of the NCI method of Yang *et al.*[6] Hirshfeld surfaces analyses were conducted with Crystal Explorer 17.5.[7]

Hirshfeld surfaces

A visual way to analyze the interactions at play in a crystal is to map the Hirshfeld surface of the system with the normalized distance d_{norm}. We refer the interested reader to Ref. 7 and recall here the main definitions only.

The Hirshfeld surface defines the volume of space in which the promolecule electron density exceeds that from all neighboring molecules. For each point of this surface, one can compute three distances:

- d_e: distance from a point on the surface to the nearest nucleus *outside* the surface
- d_i: distance from a point on the surface to the nearest nucleus *inside* the surface
- $d_{norm} = \frac{d_i - r_i^{vdW}}{r_i^{vdW}} + \frac{d_e - r_e^{vdW}}{r_e^{vdW}}$, where r_e^{vdW} is the van der Waal radius of the nearest nucleus *outside* the surface and r_i^{vdW} is the van der Waal radius of the nearest nucleus *inside* the surface.

In the following, the same color code will be used for d_{norm}: from red (distances shorter than sum of vdW radii) through white to blue (distances longer than sum of vdW radii), as illustrated in Figure S-7 below.

Figure S-7: Color code for Hirshfeld surfaces mapped with d_{norm}.

References

1) Gaussian 16, Revision **B.01**, M. J. Frisch, G. W. Trucks, H. B. Schlegel, G. E. Scuseria, M. A. Robb, J. R. Cheeseman, G. Scalmani, V. Barone, G. A. Petersson, H. Nakatsuji, X. Li, M. Caricato, A. V. Marenich, J. Bloino, B. G. Janesko, R. Gomperts, B. Mennucci, H. P. Hratchian, J. V. Ortiz, A. F. Izmaylov, J. L. Sonnenberg, D. Williams-Young, F. Ding, F. Lipparini, F. Egidi, J. Goings, B. Peng, A. Petrone, T. Henderson, D. Ranasinghe, V. G. Zakrzewski, J. Gao, N. Rega, G. Zheng, W. Liang, M. Hada, M. Ehara, K. Toyota, R. Fukuda, J. Hasegawa, M. Ishida, T. Nakajima, Y. Honda, O. Kitao, H. Nakai, T. Vreven, K. Throssell, J. A. Montgomery, Jr., J. E. Peralta, F. Ogliaro, M. J. Bearpark, J. J. Heyd, E. N. Brothers, K. N. Kudin, V. N. Staroverov, T. A. Keith, R. Kobayashi, J. Normand, K. Raghavachari, A. P. Rendell, J. C. Burant, S. S. Iyengar, J. Tomasi, M. Cossi, J. M. Millam, M. Klene, C. Adamo, R. Cammi, J. W. Ochterski, R. L. Martin, K. Morokuma, O. Farkas, J. B. Foresman, and D. J. Fox, Gaussian, Inc., Wallingford CT, **2016**.

2) Y. Zhao and D. G. Truhlar, *Theor. Chem. Acc.* **2008**, *120,* 215-41.

3) T. H. Dunning Jr., *J. Chem. Phys.* **1989**, *90,* 1007-23.

4) CYLview, 1.0b; Legault, C. Y., Université de Sherbrooke, **2009** (http://www.cylview.org). Last visited 20 June 2020.

5) a) C. Lefebvre, G. Rubez, H. Khartabil, J.-C. Boisson, J. Contreras-García, E. Hénon, *Phys. Chem. Chem. Phys.* **2017**, *19* (27), 17928–17936. b) C. Lefebvre, H. Khartabil, J.-C. Boisson, J. Contreras-Garcia, J.-P. Piquemal, J.-P.; E. Hénon, *ChemPhysChem* **2018**, 19, 1.

6) E. R. Johnson, S. Keinan, P. Mori-Sánchez, J. Contreras-García, A. J. Cohen, W. Yang, *J. Am. Chem. Soc.* **2010**, *132*, 6498–6506.

7) a) Spackman, M. A.; Jayatilaka, D. Hirshfeld surface analysis. CrystEngComm 2009, 11, 19−32; b) Spackman, M. A.; McKinnon, J. J.; Jayatilaka, D. Electrostatic potentials mapped on Hirshfeld surfaces provide direct insight into intermolecular interactions in crystals. CrystEngComm 2008, 10, 377−388. c) https://crystalexplorer.scb.uwa.edu.au/. Last visited July, 10th 2020.

Compound 1Br

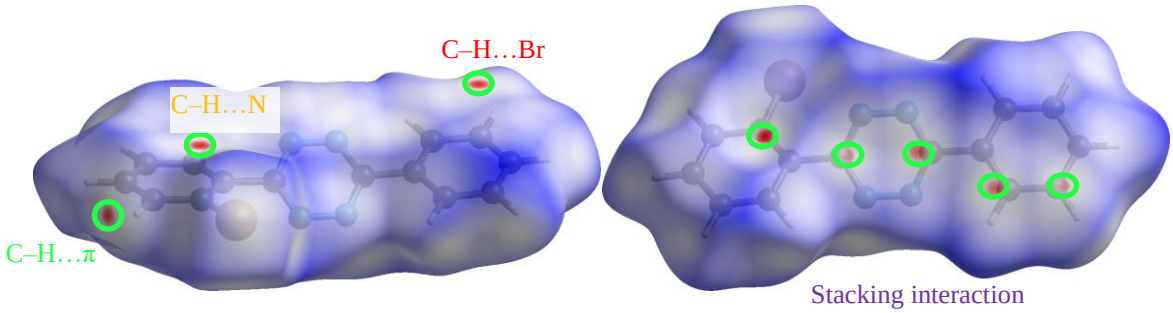

Figure S-8: Hirshfeld surfaces mapped with d_{norm}. left: front view, right: back view.

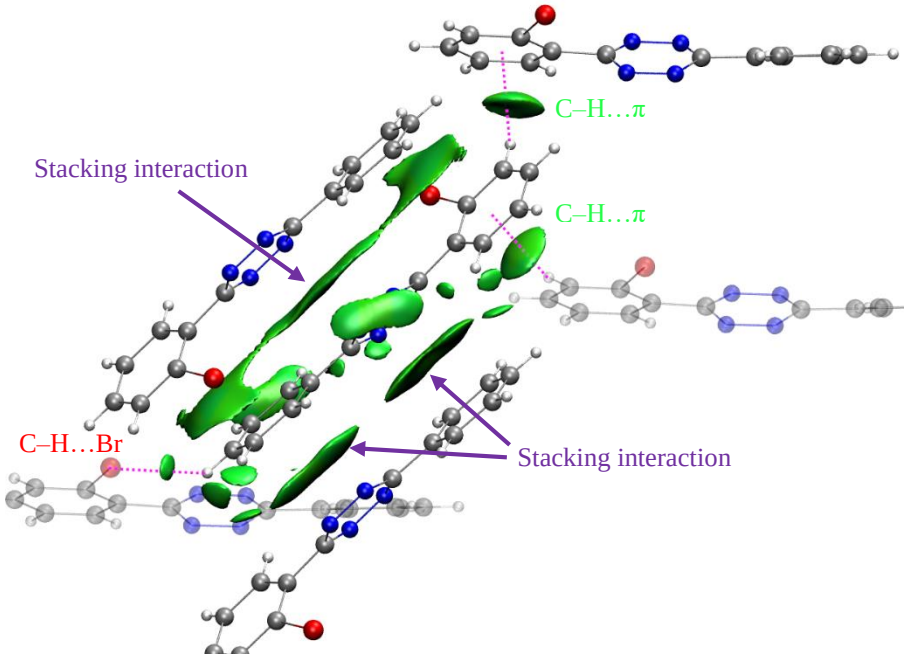

Figure S-9: Non-Covalent interactions illustrating stacking interactions (purple), C–H…Br interactions (red) and C–H…π interactions (green). Color code: carbon in grey, nitrogen in blue, hydrogen in white and bromine in red.

Compound 2

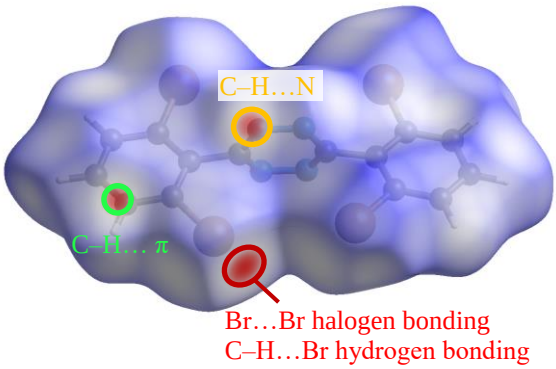

Figure S-10: Hirshfeld surfaces mapped with d_{norm}.

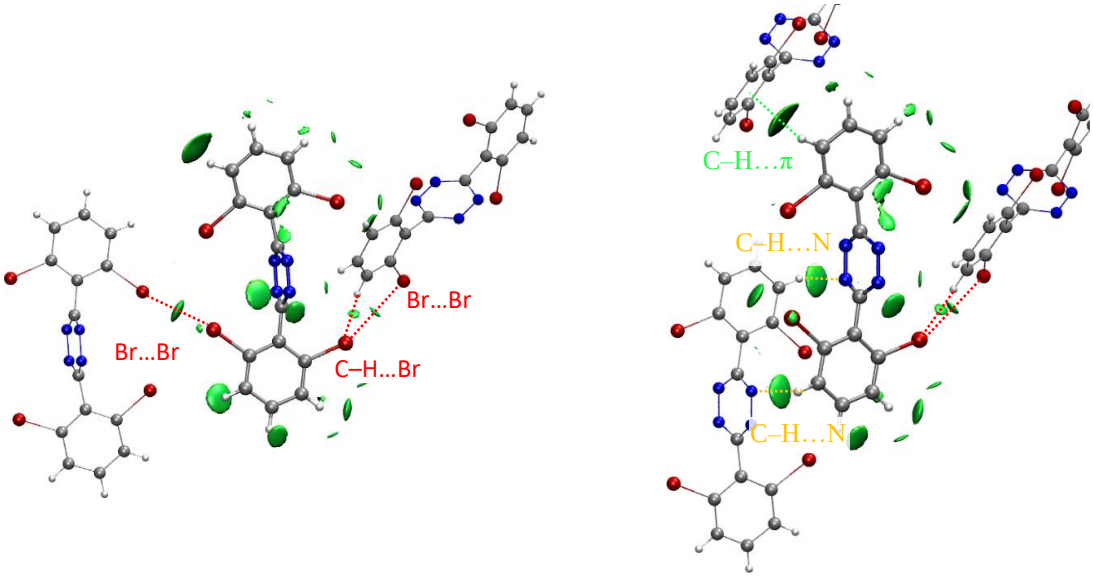

Figure S-11: Non-covalent interactions for Compound 2. Left: Halogen Br-Br bonds and CH-Br bond; Right: CH-Br and Br-Br interactions (red), CH-N interactions (orange) and CH-π interactions (green). Color code: carbon in grey, nitrogen in blue, hydrogen in white and bromine in red.

Molecular Electrostatic Potential

The molecular electrostatic potential for compound **2** is shown Fig. S-12.

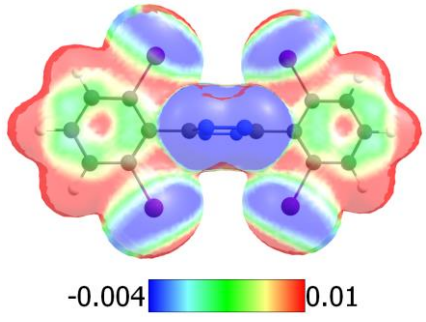

Figure S-12: Molecular Electrostatic Potential for compound **2**.

When superimposed with the X-ray structure (Fig SX2), it shows the favorable electrostatic interactions between the negatively charged lone pairs of the tetrazine core and the positively charged C–H bonds of the electron-poor dibromophenyl groups.

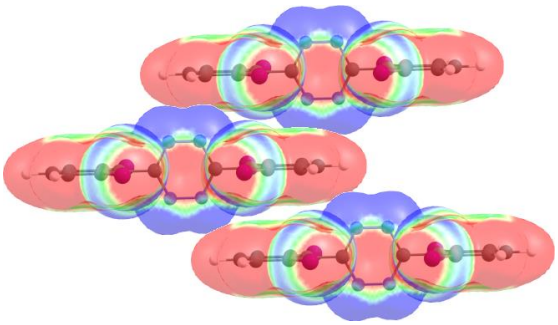

Figure S-13: MEP of compound **2** superimposed on the X-ray structure.

Distorted geometry stability

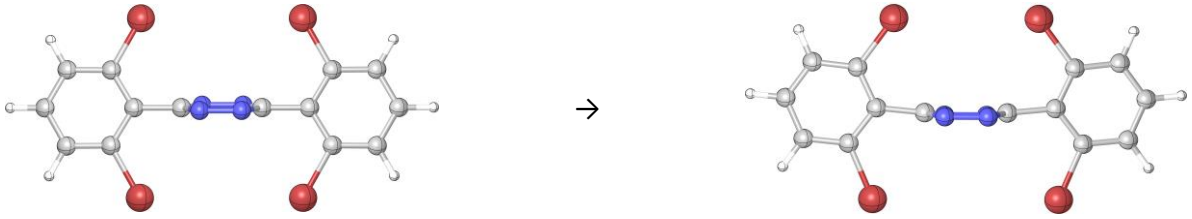

E = 0.00 Kcal mol^{-1} E = 0.54 Kcal mol^{-1}

Figure S-14: Distortion of tetrazine core of compound **2**. Electronic energies at the M06-2X/aug-cc-pVTZ level.

Compound 3

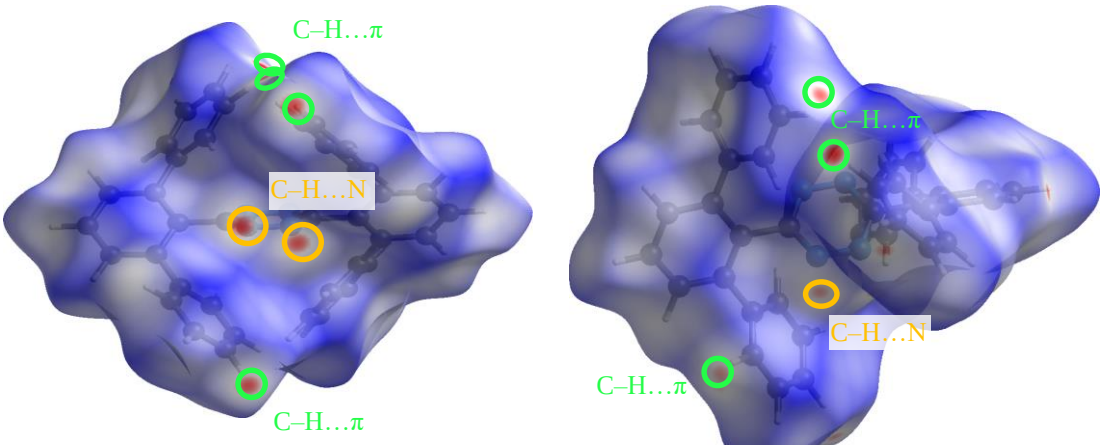

Front view Side view

Figure S-15: Hirshfeld surfaces for **3** conformer **A'** mapped with d_{norm} (left: front view, right: back view)

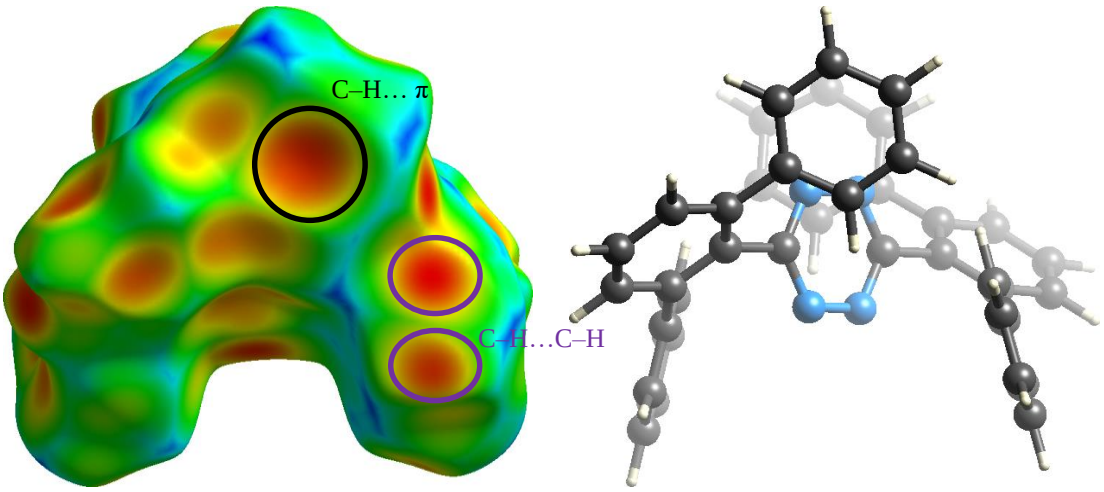

a) Hirshfeld surface mapped with d_e b) Conformer **A'**

Figure S-16: Hirshfeld surfaces for compound **3** conformer **A'** mapped with d_e. Color code for d_e: red (short distances) through green to blue (long distances). Color code: carbon in grey, nitrogen in blue, hydrogen in white.

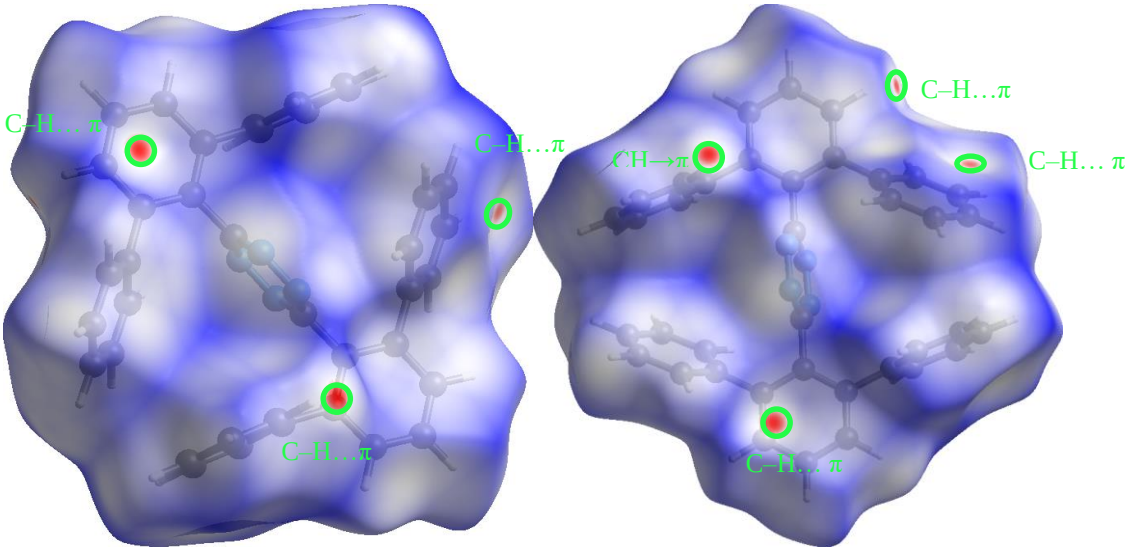

Figure S-17: Hirshfeld surfaces for compound **3** conformer **B'** mapped with d_{norm} (left: front view, right: back view).

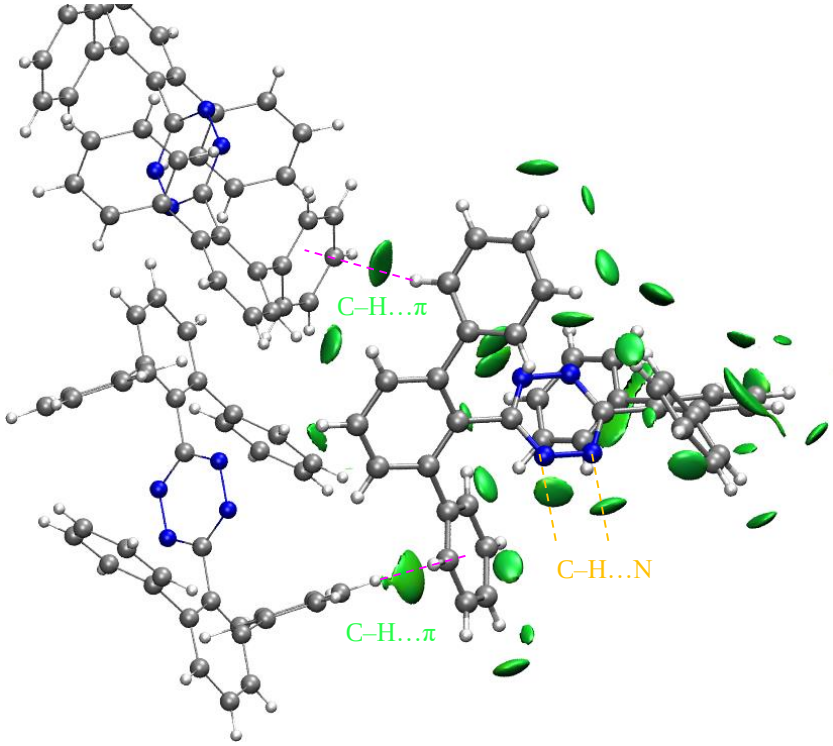

Figure S-18: Non Covalent interactions map showing the CH-π interactions between **A'** (large ball & stick) and **B'** molecules (slim ball & stick). Color code: carbon in grey, nitrogen in blue, hydrogen in white.

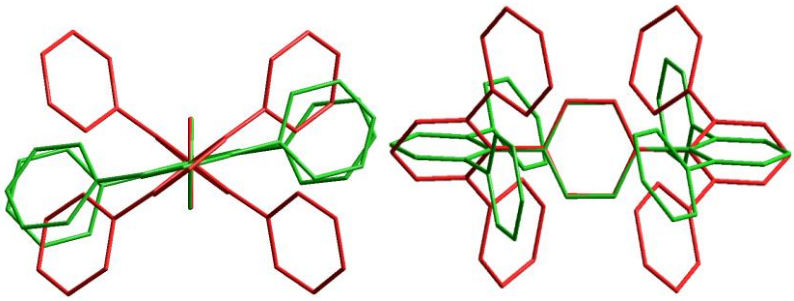

Figure S-19: Superimposed views of **3** conformers **A'** and **B'**. Left: front view, Right: top view. Isomer **A'** is shown in red and isomer **B'** in green.

Compound 4

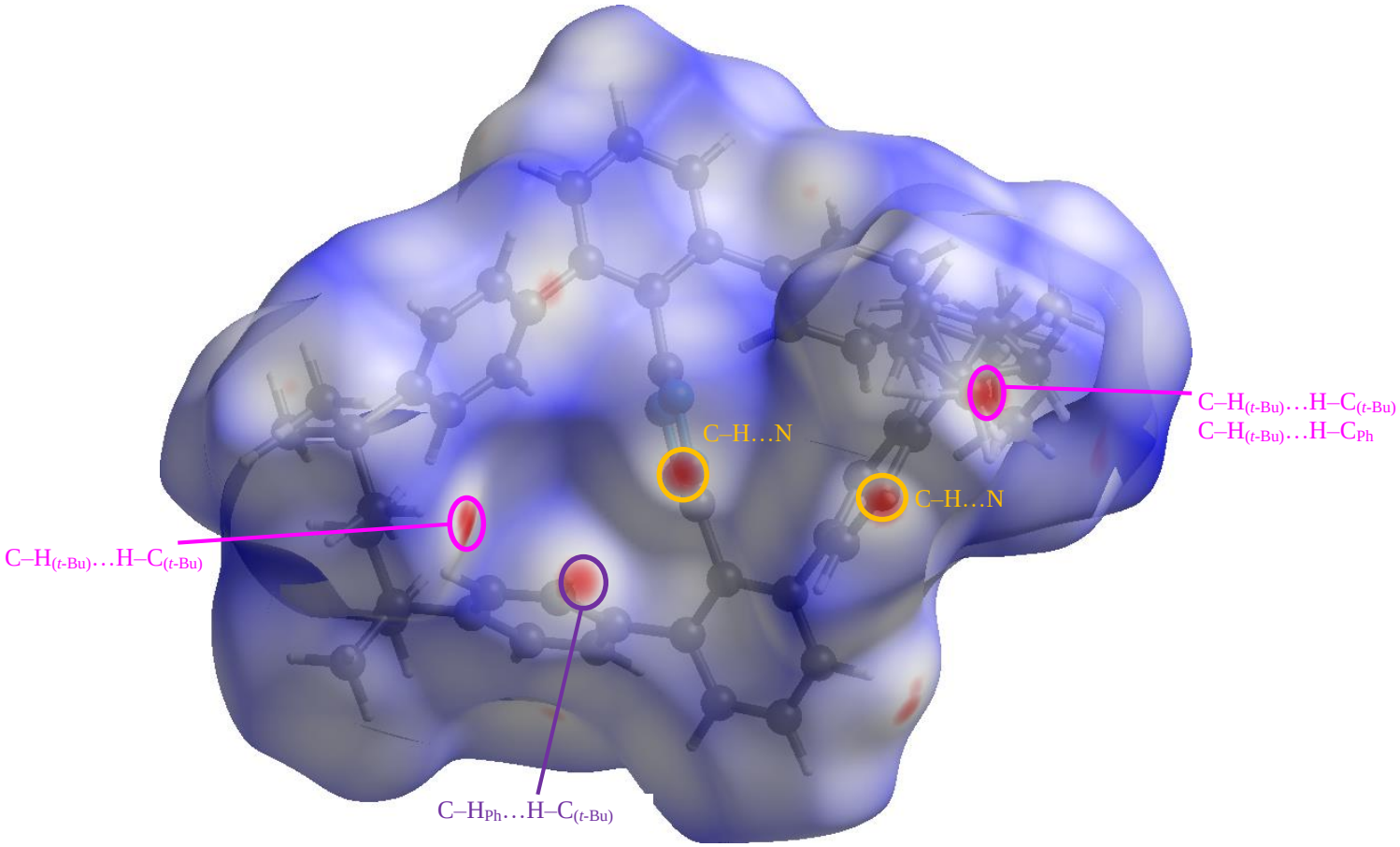

Figure S-20: Hirshfeld surfaces for compound **4** mapped with d_{norm}.

Compound 10

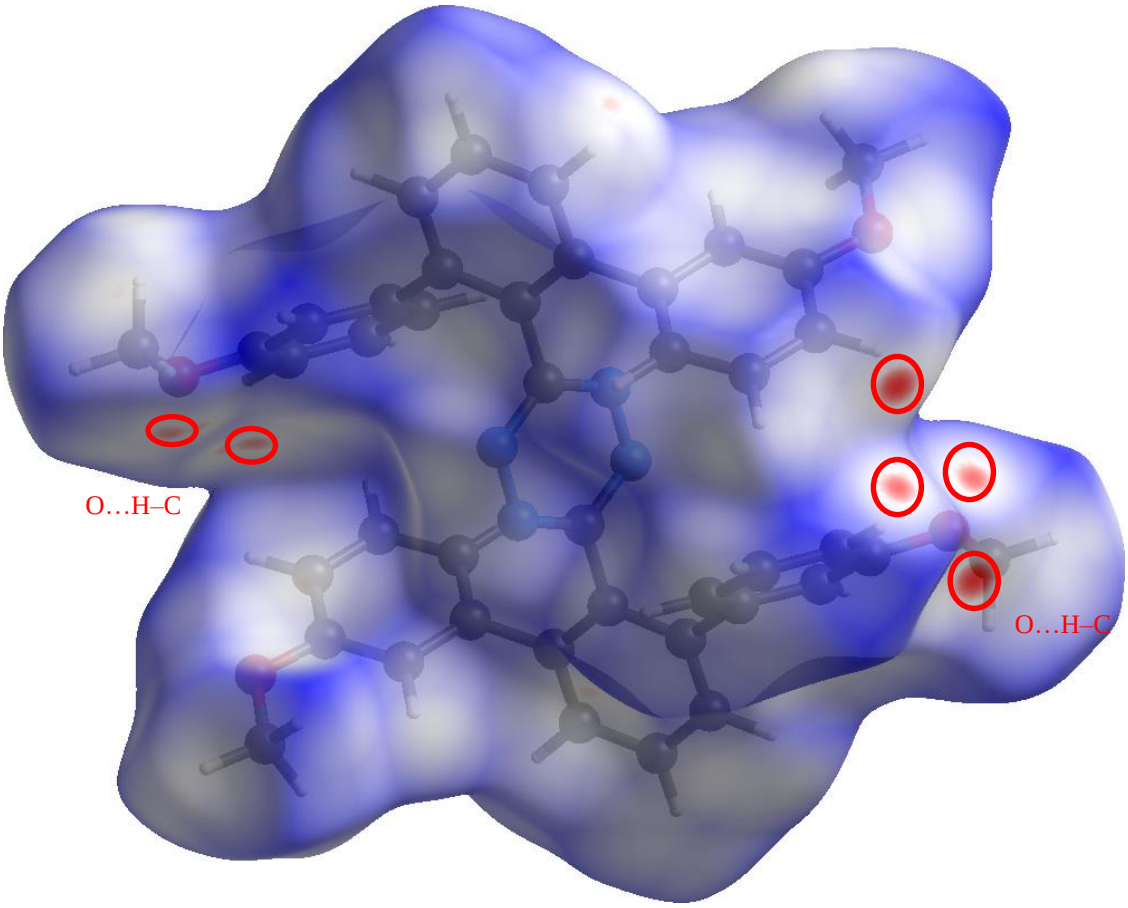

Figure S-21: Hirshfeld surfaces for compound **10** mapped with d_{norm}.

List of inter and intra-molecular interactions

Table S-5: List of inter and intra-molecular interactions

Compound	Type of interactions		Distances (Å)	Angle (°)
1-Br (Figure 2)	intermolecular interactions between aromatic moieties	**Ct1-Ct3^{i}** Ct1 = C1(Br)–C2–C3–C4–C5–C6 Ct3^{i} = C9^{i}–C10^{i}–C11^{i}–C12^{i}–C13^{i}–C14^{i} with i : 1-x, 1-y, 1-z	3.8547(13)	
		Ct2-Ct2^{i} Ct2 = C7–N1–N2–N3–N4–C8 Ct2^{i} = C7^{i}–N1^{i}–N2^{i}–N3^{i}–N4^{i}–C8^{i} with i : 1-x, 1-y, 1-z	4.1285(11)	
	Hydrogen intermolecular interactions C–H···N	C5–H5···N2^{ii} with ii : x, 1/2-y, 1/2+z	3.658(3)	141.20(13)
		C14–H14···N3^{iii} with iii : x, 1/2-y, -1/2+z	3.411(13)	131.78(14)
		C13–H13···N4^{iii} with iii : x, 1/2-y, -1/2+z	3.487(3)	137.12(15)
2 (Figure 3)	intermolecular interactions between aromatic moieties	**Ct3-Ct3^{i}** Ct3 = C9–C10(Br3)–C11–C12–C13–C14(Br4) Ct3^{i} = C9^{i}–C10^{i}(Br3)–C11^{i}–C12^{i}–C13^{i}–C14^{i}(Br4) with i : -x, 1-y, 1-z	3.7292(15)	
	Hydrogen intermolecular interactions C–H···N	C12–H12···N2^{i} with i : -x, 1-y, 1-z	3.247(3)	109.23(16)
		C13–H13···N3^{ii} with ii : 1-x, 1-y, 1-z	3.091(3)	105.36(16)
3 A' (Figure 6, bottom)	Hydrogen intermolecular interactions C–H···N	C10–H10···N2^{iv} with iv : x, 2-y, 1/2+z	3.357(3)	139.50(15)
		C17–H17···N1^{viii} with viii : x, 1-y, -1/2+z	3.373(3)	134.66(11)
3 B' (Figure 9)	Hydrogen intramolecular interactions C–H···N	C28–H28···N3^{ii} with ii : 1/2-x, 1/2-y, 1-z	3.287(3)	122.79(14)
		C12–H12···N3^{i} with i : 1-x, 1-y, -z	3.442(3)	155.83(15)

4 (Figure 11)	Hydrogen intermolecular interactions C–H···N	C22–H22···N1^{ii} with ii : 1-x, 1-y, 1-z	3.527(3)	167.26(14)
10 (Figure 13)	Hydrogen intermolecular interactions C–H···N	C21–H21···N2^{v} with v : 1+x, y, z	3.7238(16)	176.41(7)
	Hydrogen intermolecular interactions C–H···O	C21–H21···O1^{v} with v : 1+x, y, z	3.3735(16)	123.25(8)
		C21–H21···O2^{ii} with ii : 2-x, 1-y, 1-z	3.4858(15)	143.03(7)

^{1}H, ^{19}F and ^{13}C NMR copy of products

3,6-di([1,1':3',1''-terphenyl]-2'-yl)-1,2,4,5-tetrazine (3)

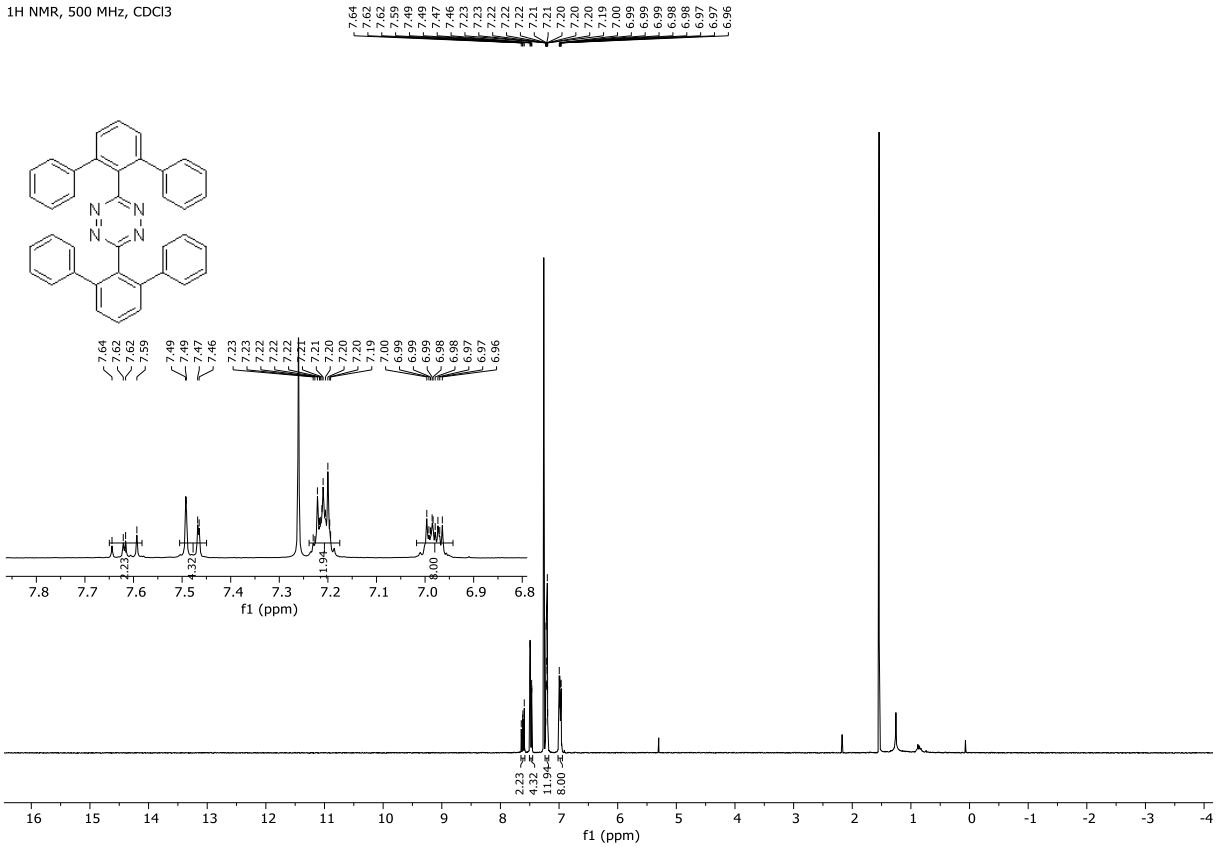

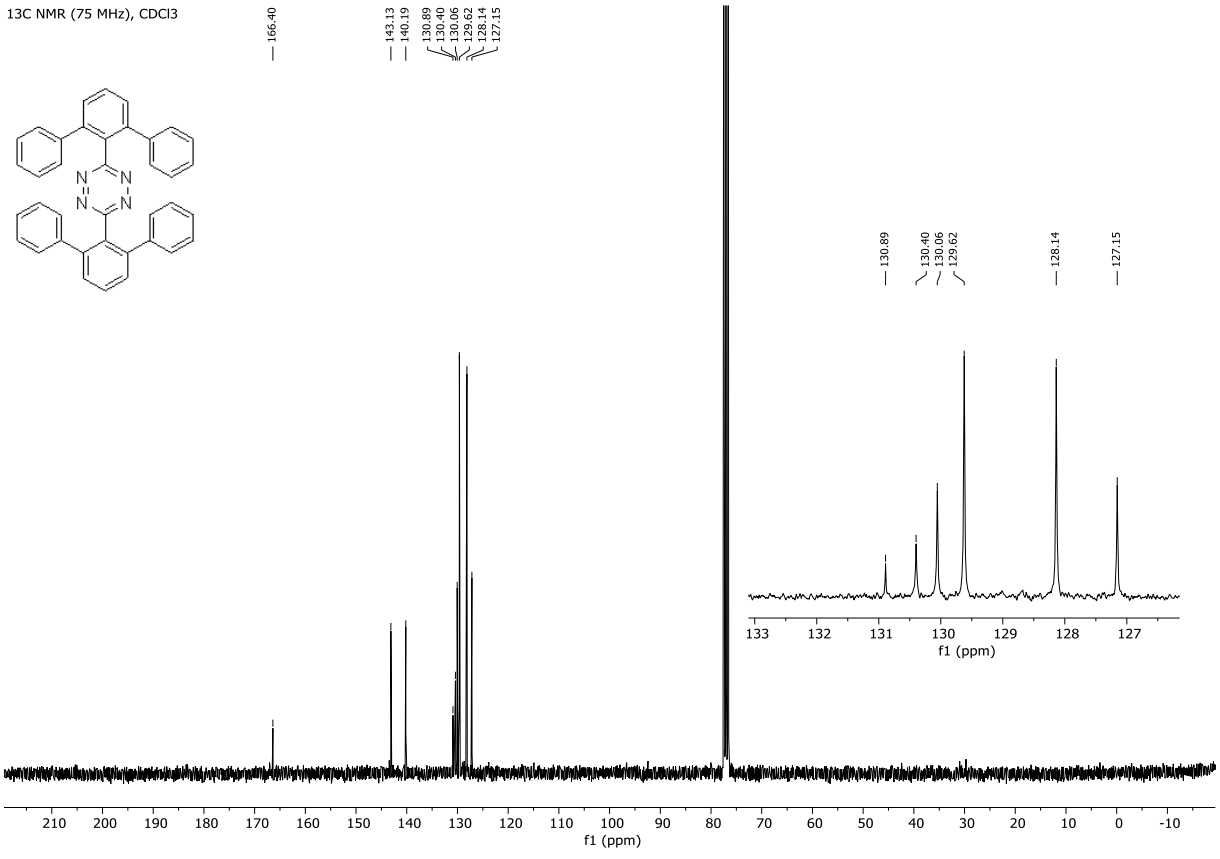

3,6-bis(4,4''-di-tert-butyl-[1,1':3',1''-terphenyl]-2'-yl)-1,2,4,5-tetrazine (4)

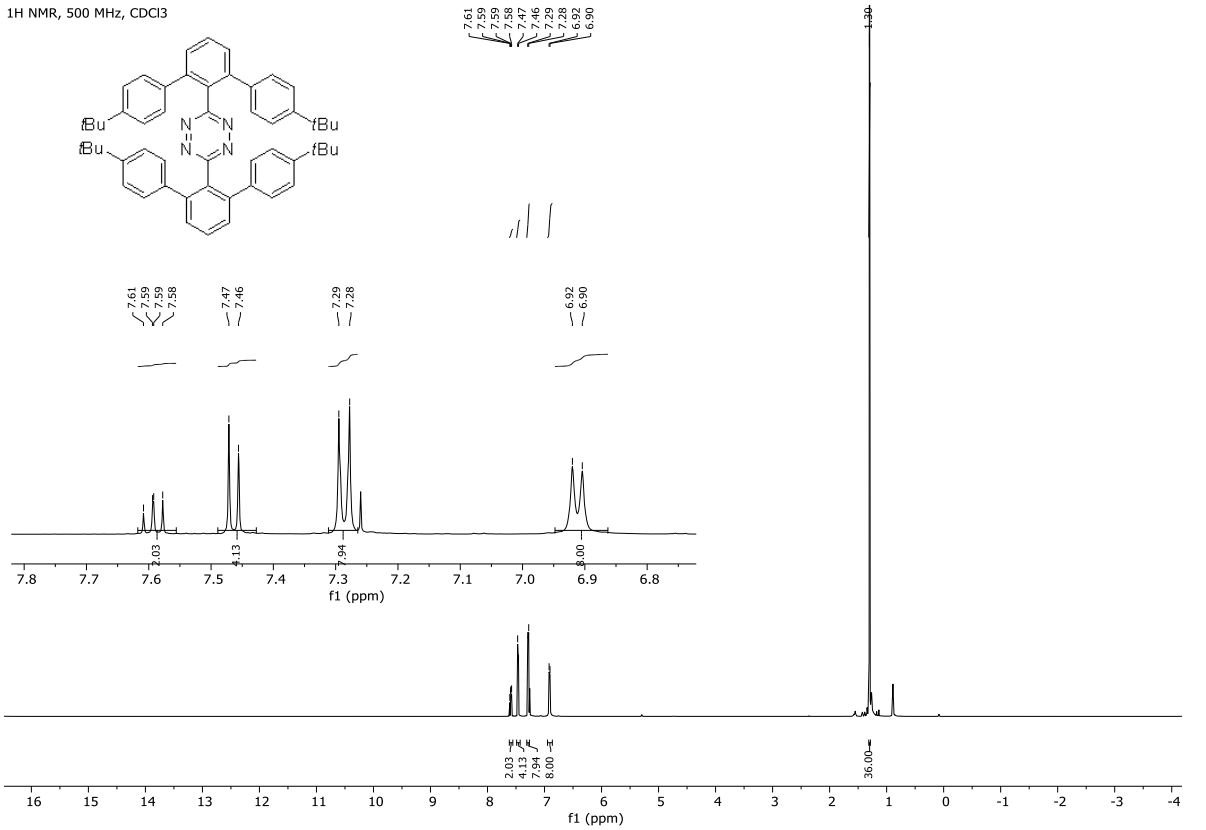

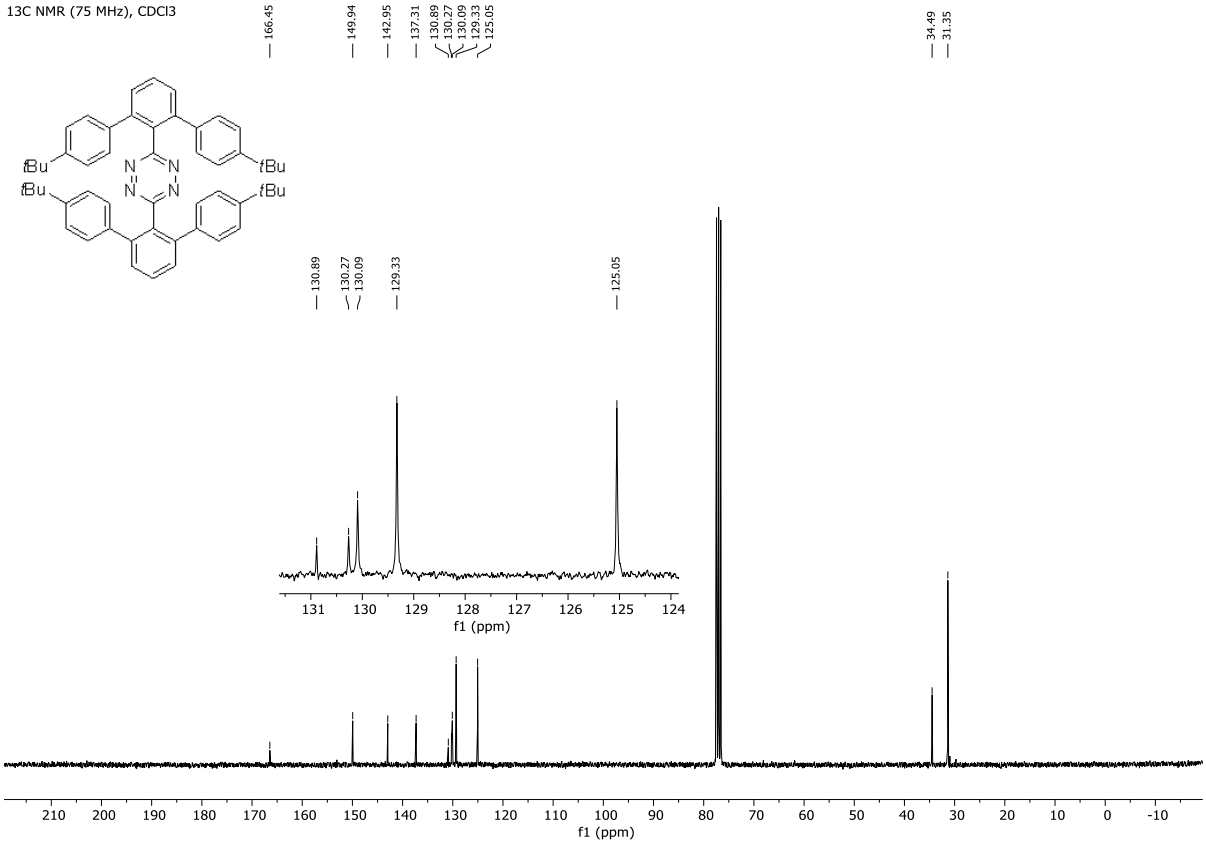

3,6-bis(4,4''-dimethoxy-[1,1':3',1''-terphenyl]-2'-yl)-1,2,4,5-tetrazine (5)

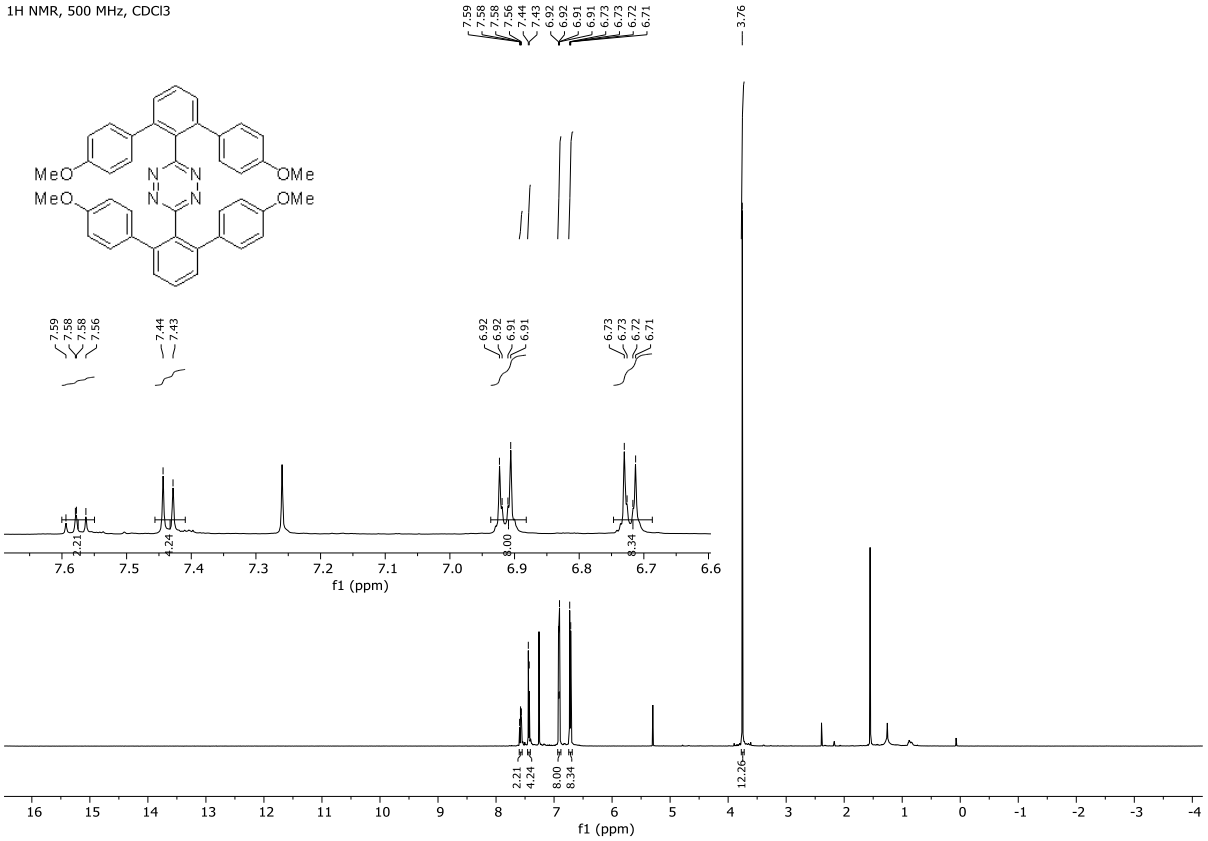

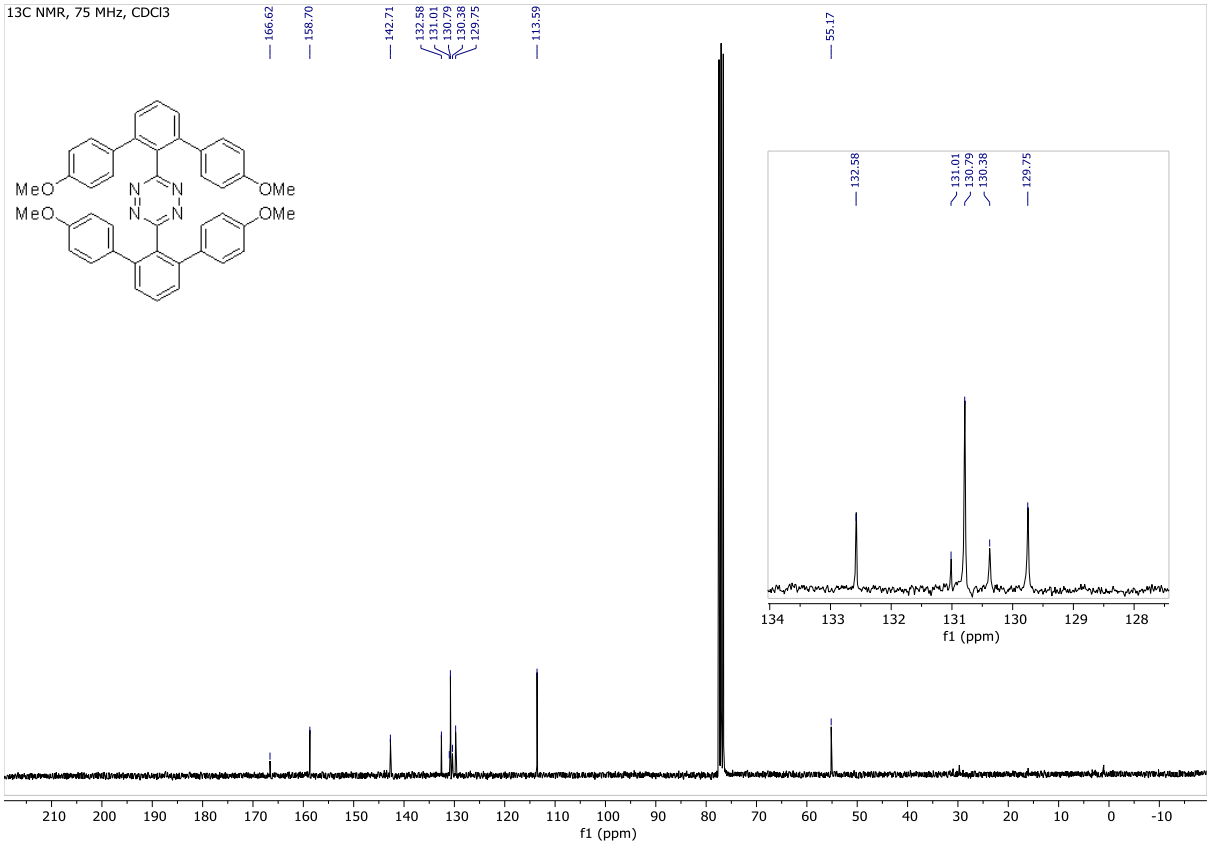

3,6-bis(4,4''-difluoro-[1,1':3',1''-terphenyl]-2'-yl)-1,2,4,5-tetrazine (6)

1H NMR, 500 MHz, CDCl3

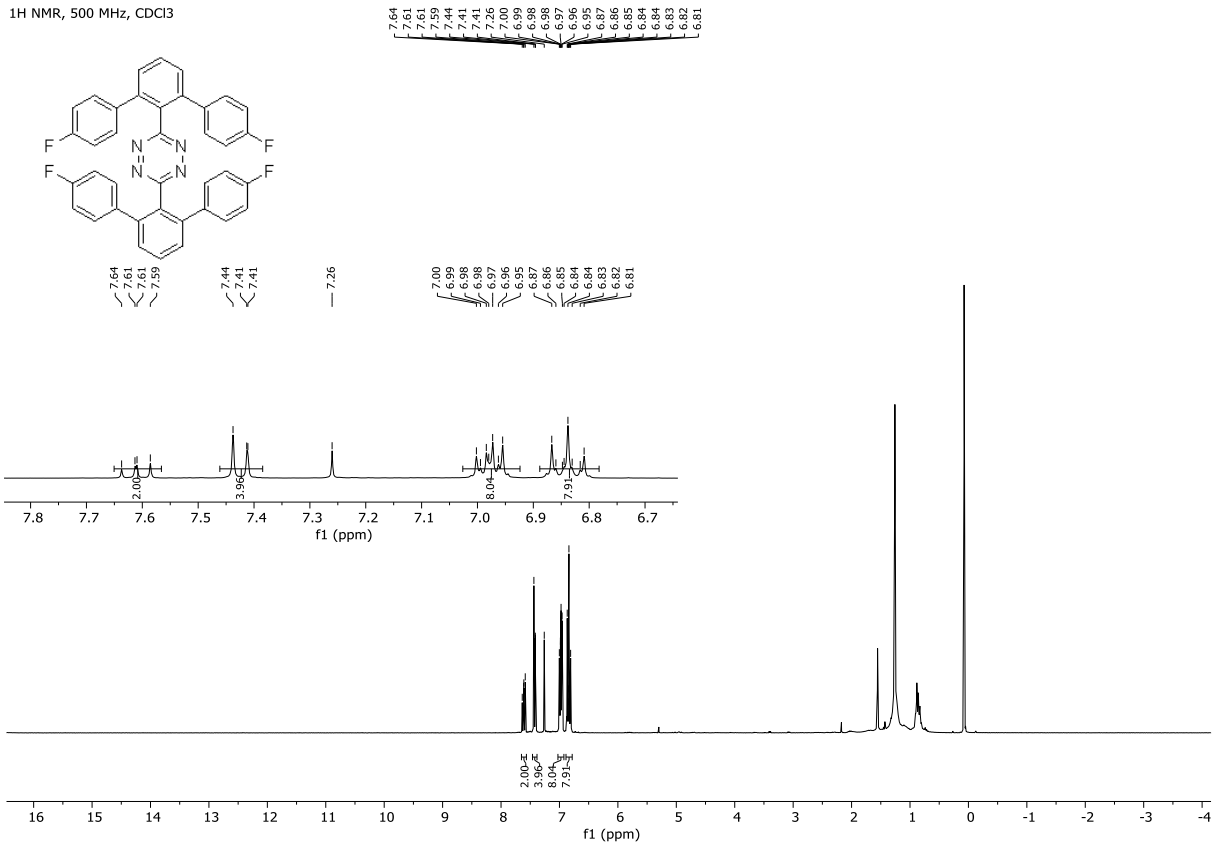

19F NMR (470 MHz), CDCl3

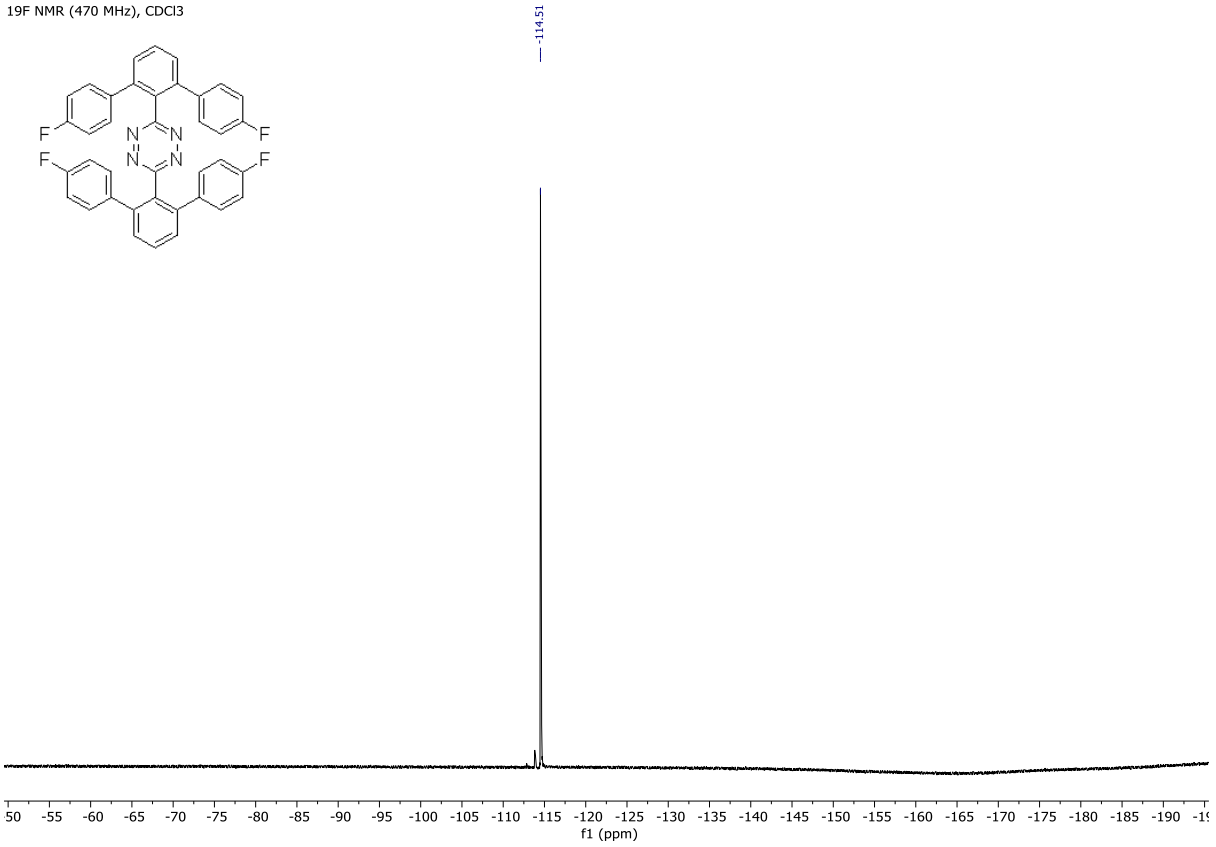

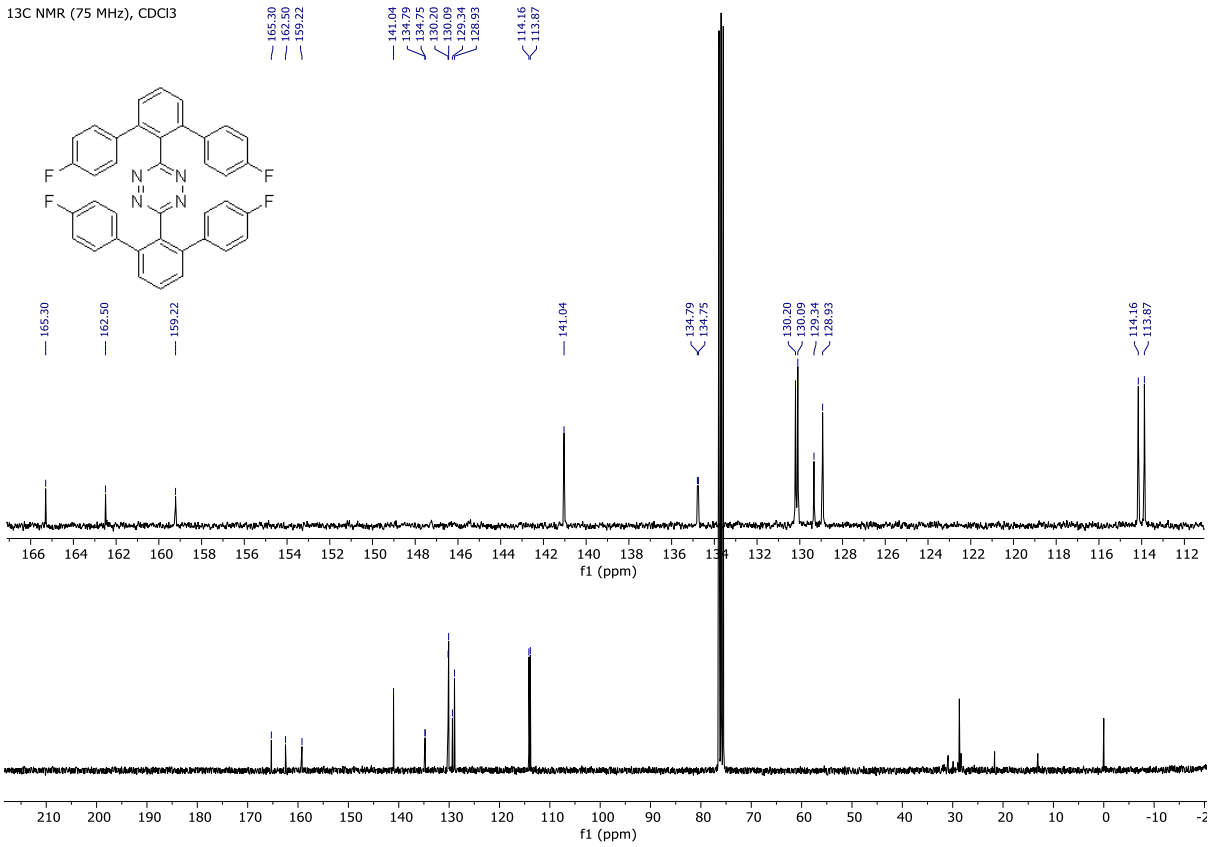
13C NMR (75 MHz), CDCl3
165.30
162.50
159.22
141.04
134.79
134.75
130.20
130.09
129.34
128.93
114.16
113.87
F
F
F
F
N
N
N
N
f1 (ppm)
f1 (ppm)

3,6-bis(4,4''-dibromo-[1,1':3',1''-terphenyl]-2'-yl)-1,2,4,5-tetrazine (7)

1H NMR, 500 MHz, CDCl3

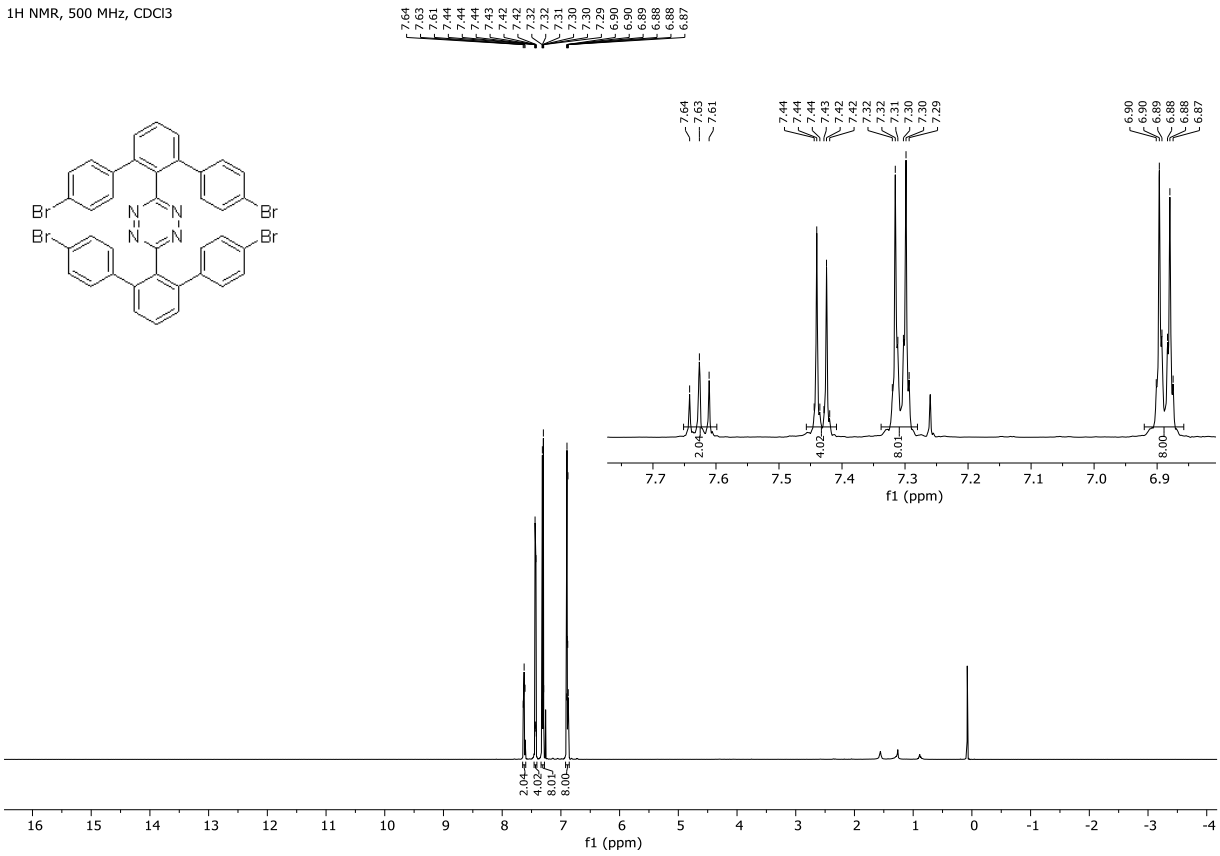

13C NMR, 125 MHz, CDCl3

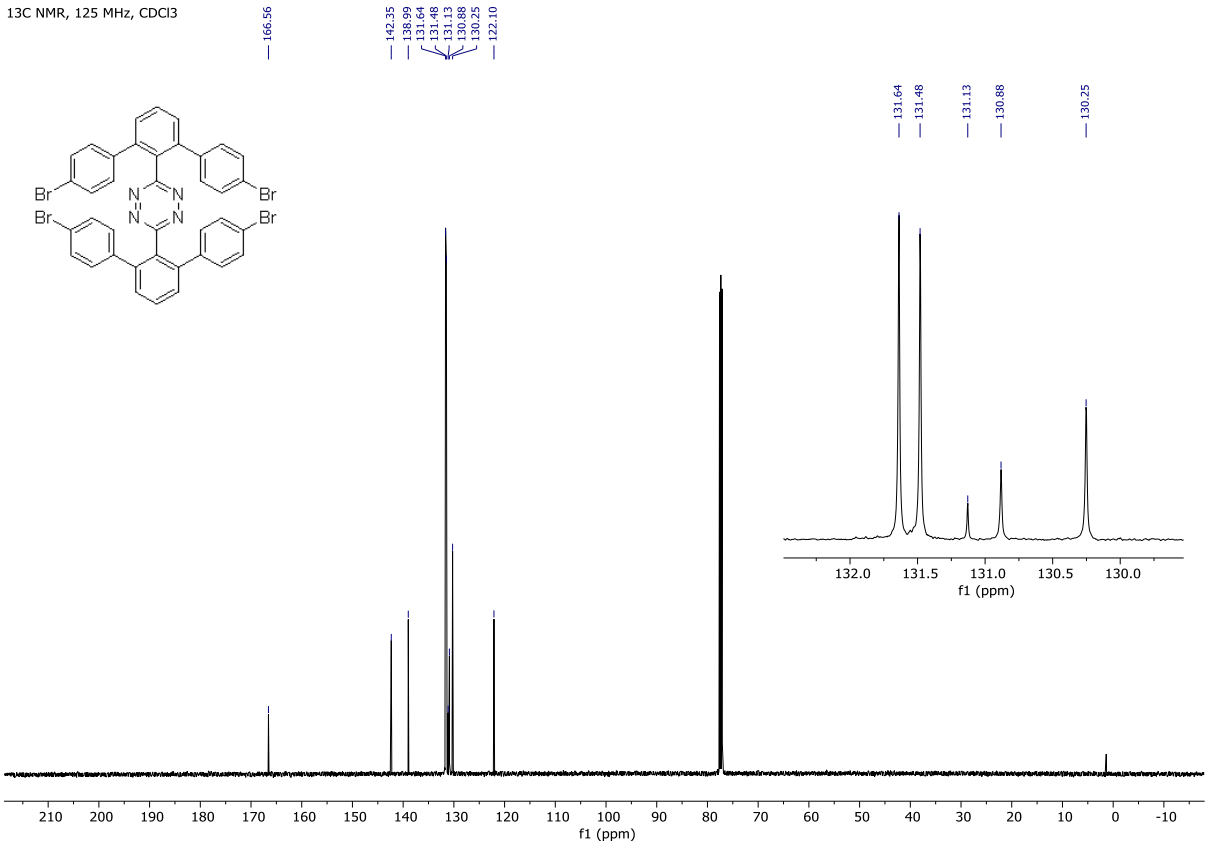

3,6-bis(4,4''-trifluoromethyl-[1,1':3',1''-terphenyl]-2'-yl)-1,2,4,5-tetrazine (8)

1H NMR (500 MHz), CDCl3

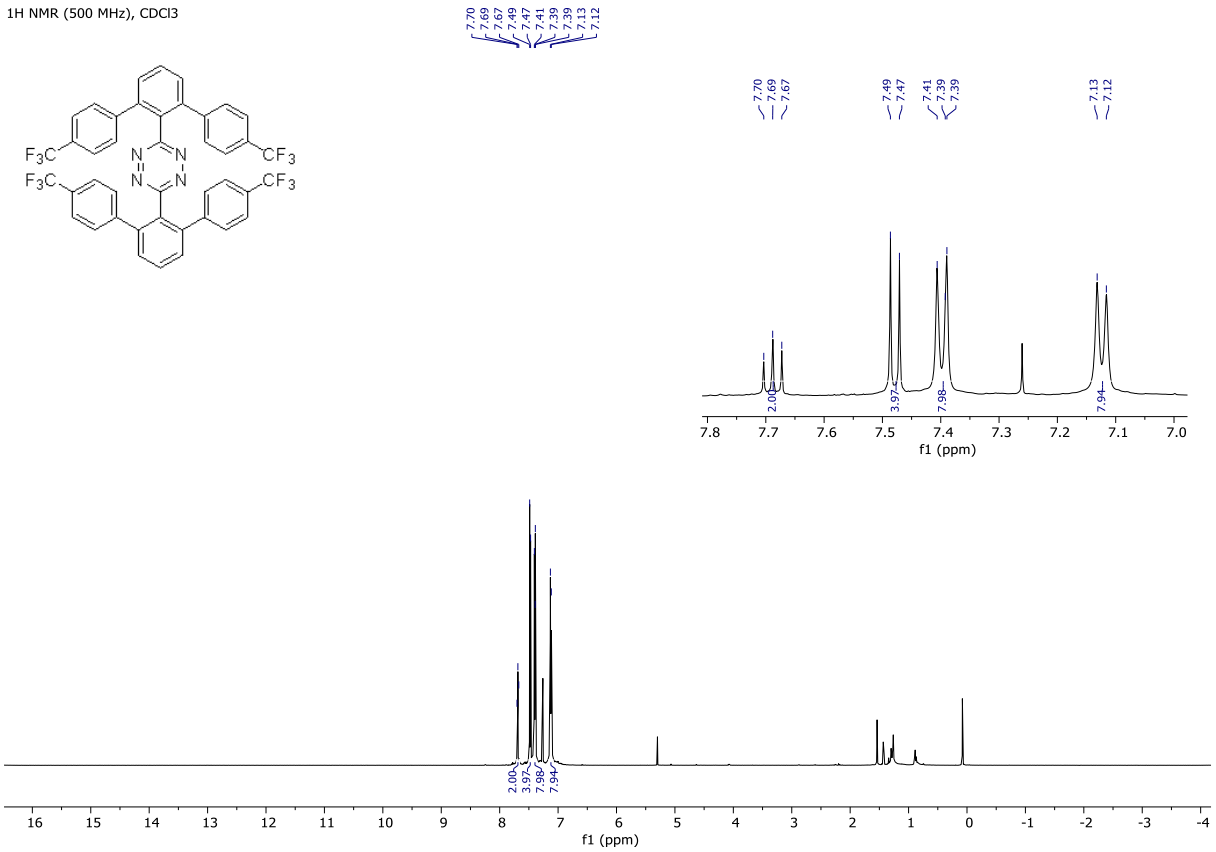

19F NMR (470 MHz), CDCl3

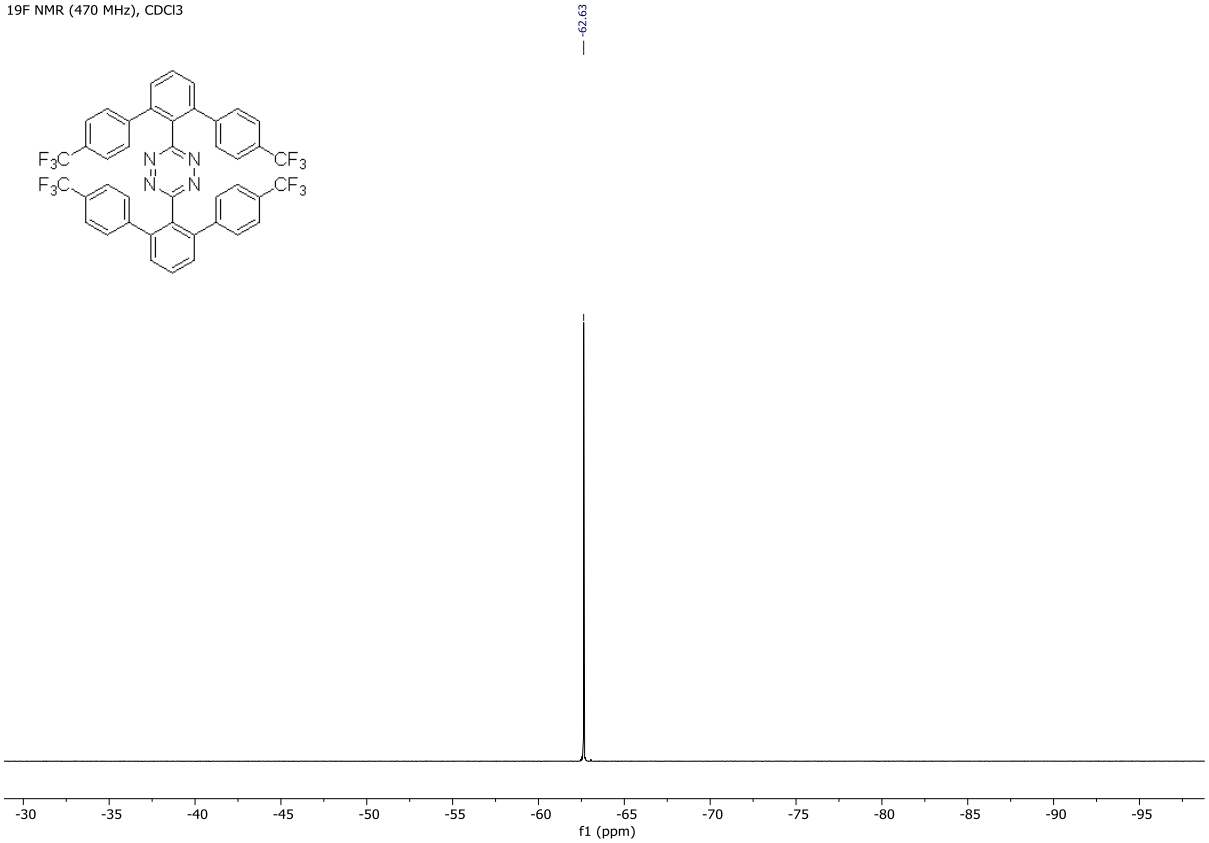

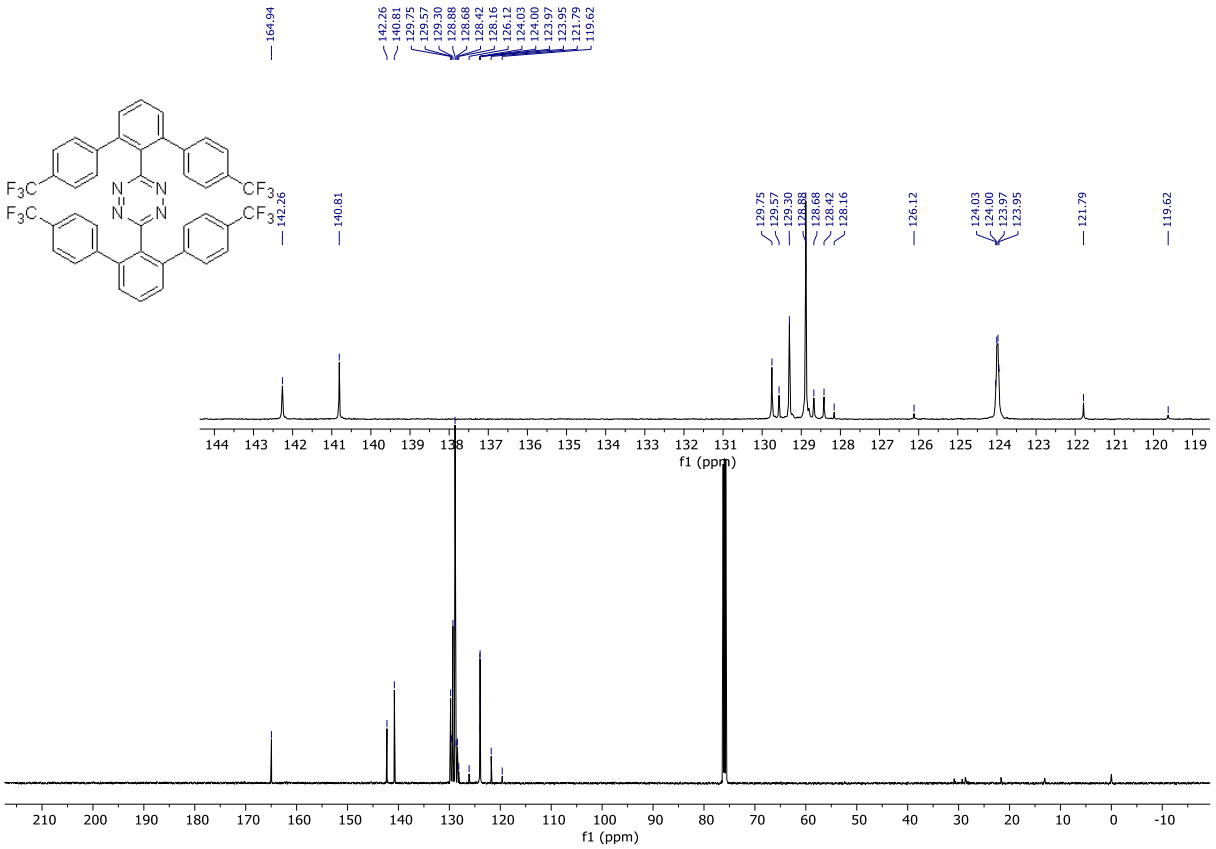
164.94
142.26
140.81
129.75
129.57
129.30
128.88
128.68
128.42
128.16
126.12
124.03
124.00
123.97
123.95
121.79
119.62
F3C
CF3
F3C
CF3
N
N
N
N
f1 (ppm)
f1 (ppm)

3,6-bis(4,4''-acetyl-[1,1':3',1''-terphenyl]-2'-yl)-1,2,4,5-tetrazine (9)

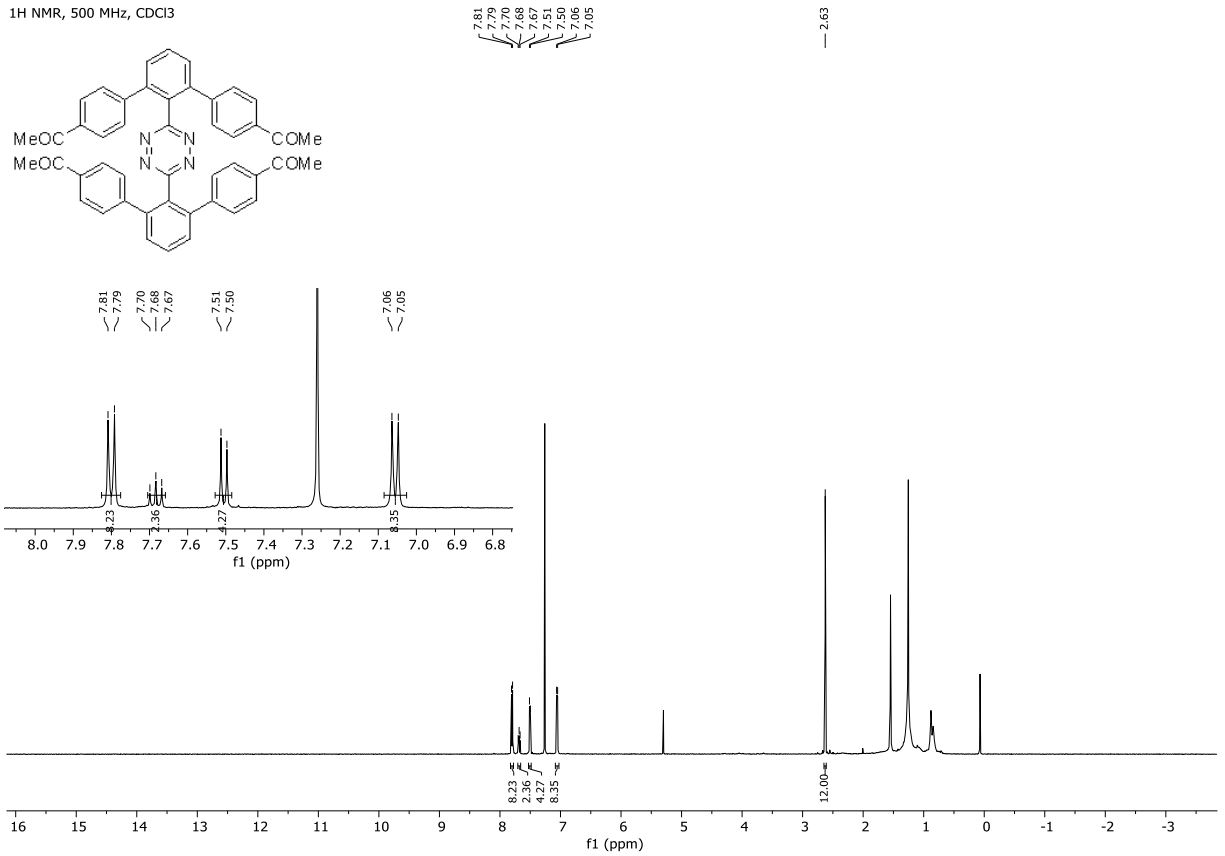

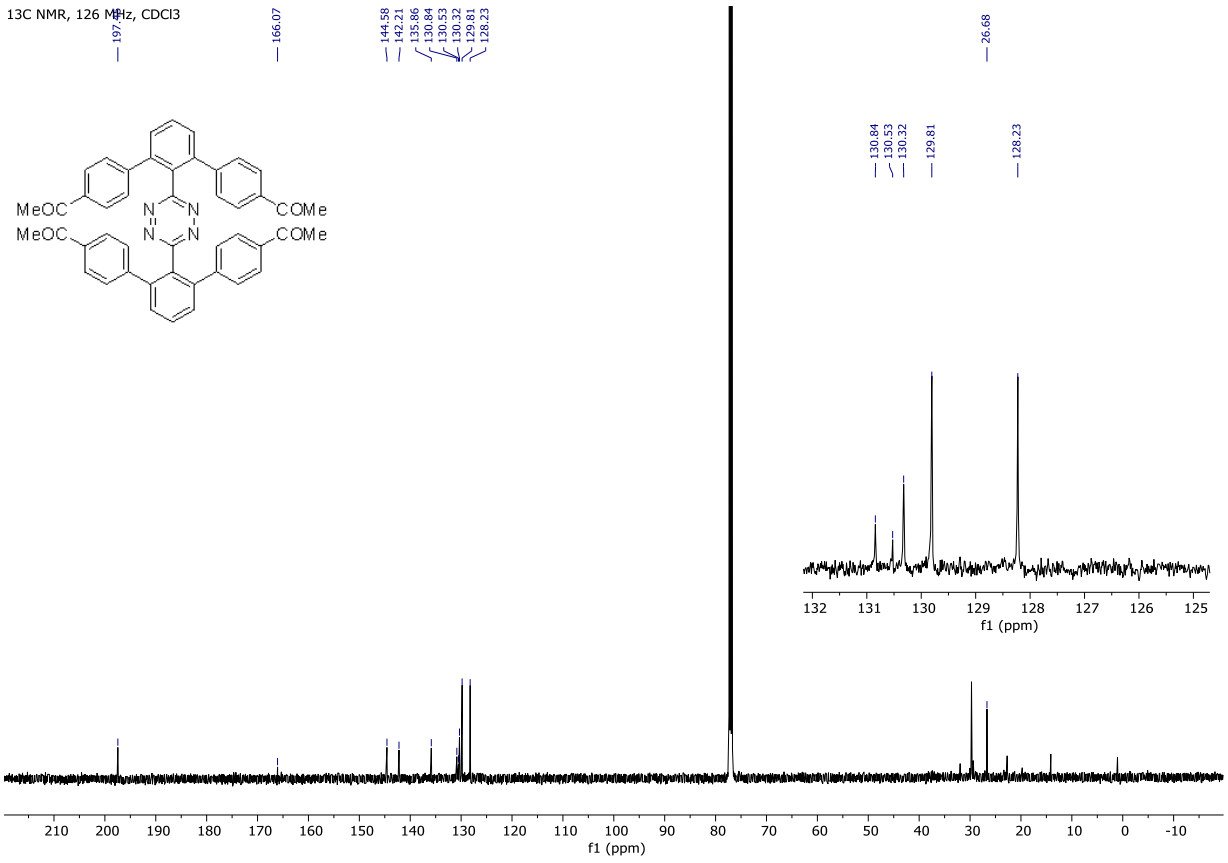

3,6-bis(3,3''-dimethoxy-[1,1':3',1''-terphenyl]-2'-yl)-1,2,4,5-tetrazine (10)

1H NMR (500 MHz), CDCl3

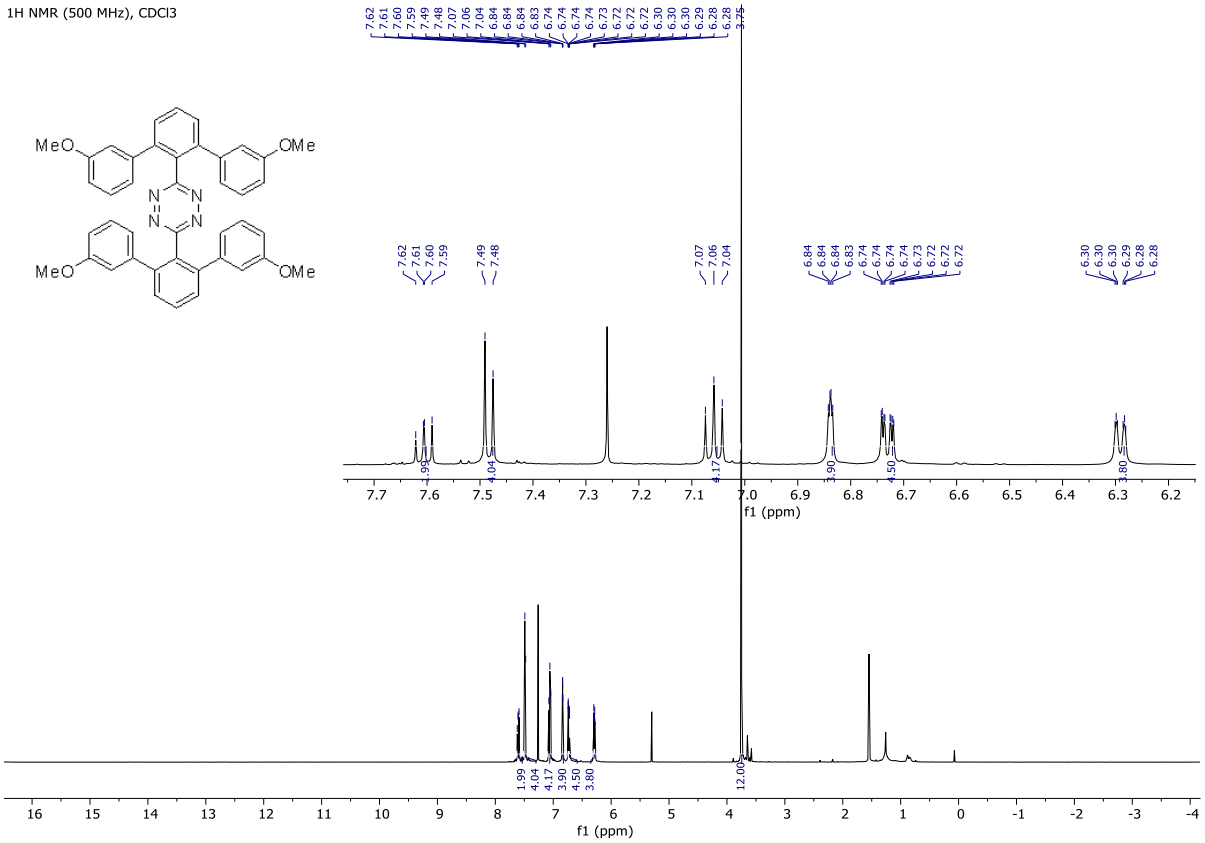

13C NMR (125 MHz), CDCl3

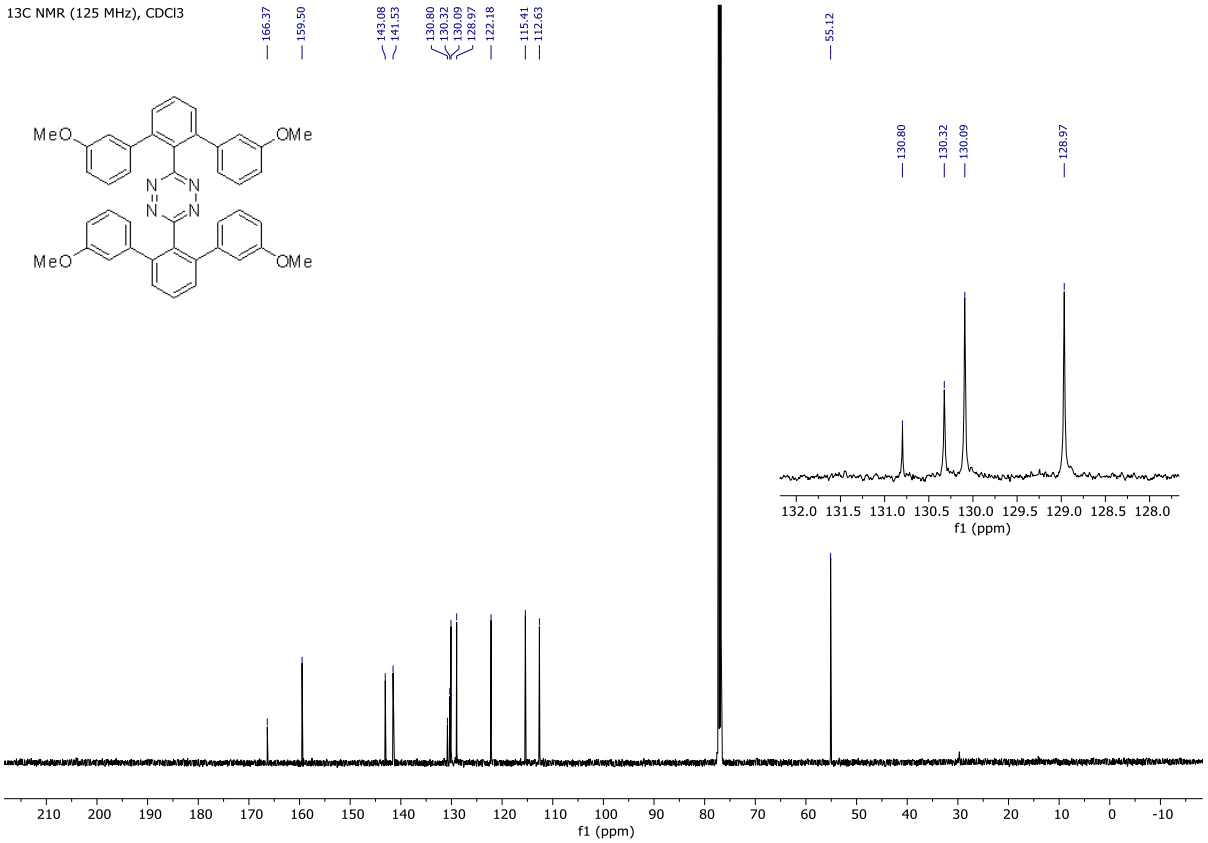

3,6-bis(3,3''-dibromo-[1,1':3',1''-terphenyl]-2'-yl)-1,2,4,5-tetrazine (11)

1H NMR, 500 MHz, CDCl3

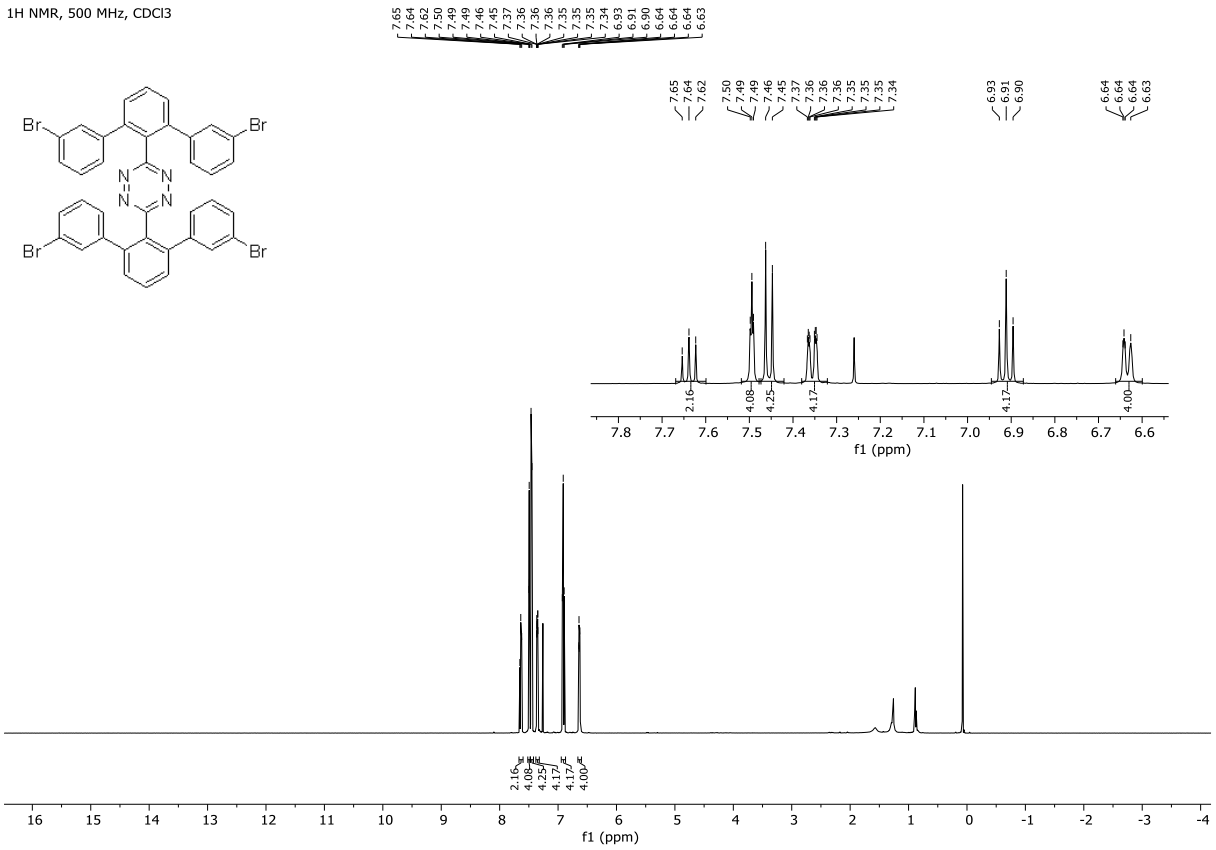

13C NMR, 125 MHz, CDCl3

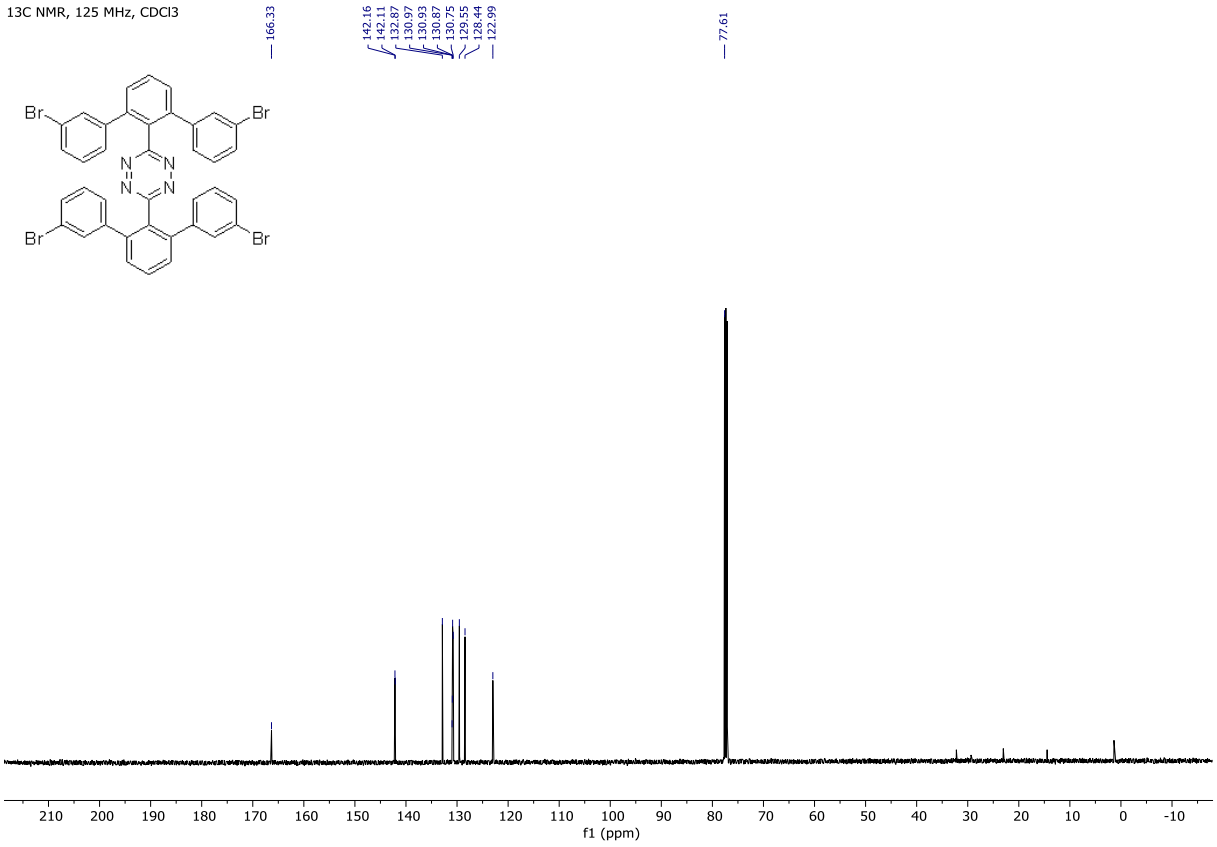

3,6-bis(2,6-di(thiophen-2-yl)phenyl)-1,2,4,5-tetrazine (13)

1H NMR (500 MHz), CDCl3

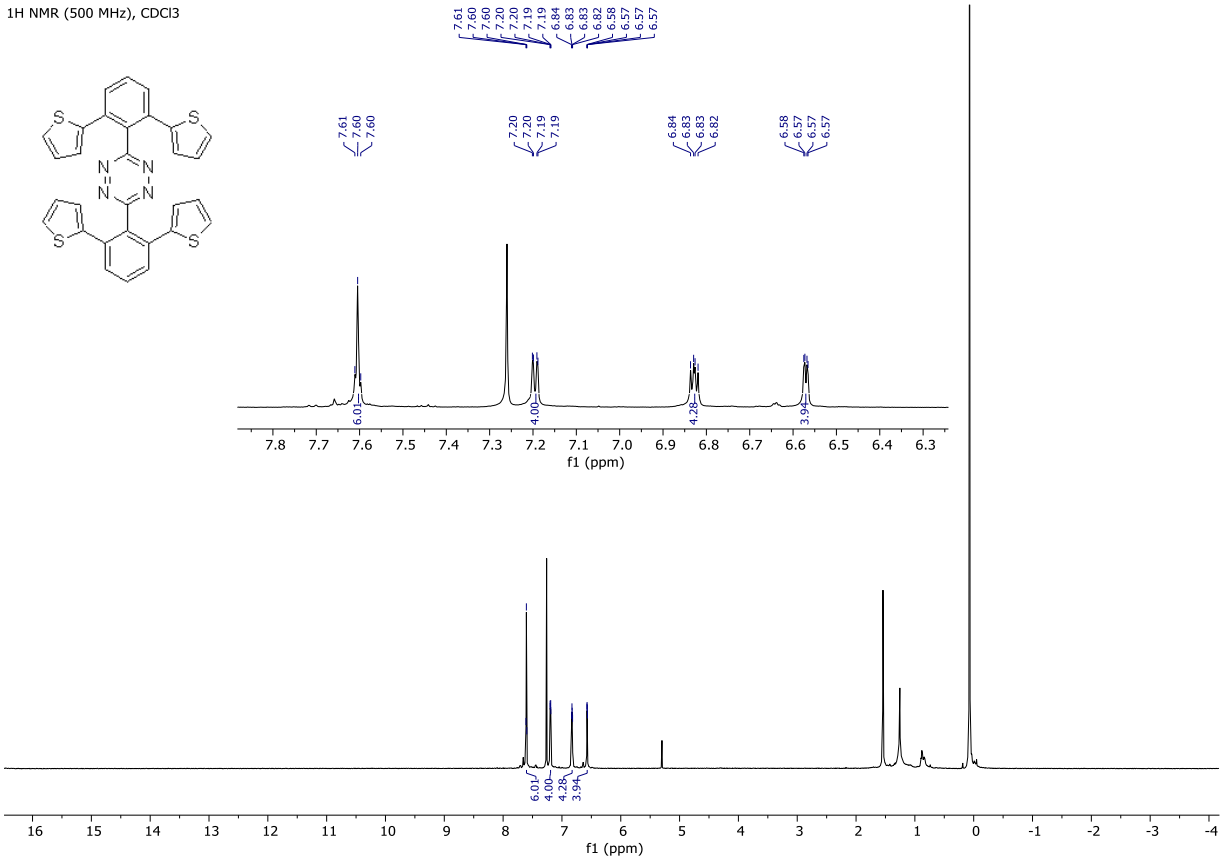

13C NMR (125 MHz), CDCl3

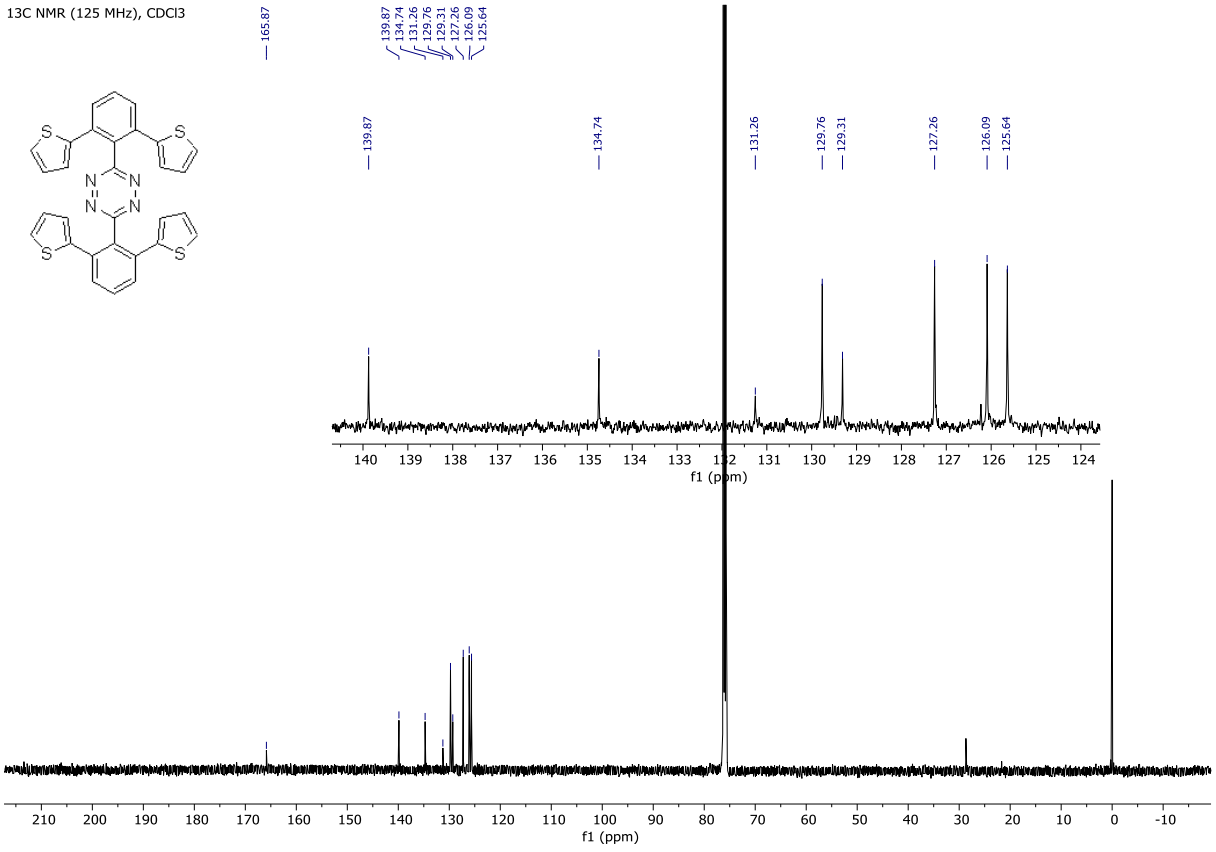

3,6-bis(2,6-di(thiophen-3-yl)phenyl)-1,2,4,5-tetrazine (13)

1H NMR (500 MHz), CDCl3

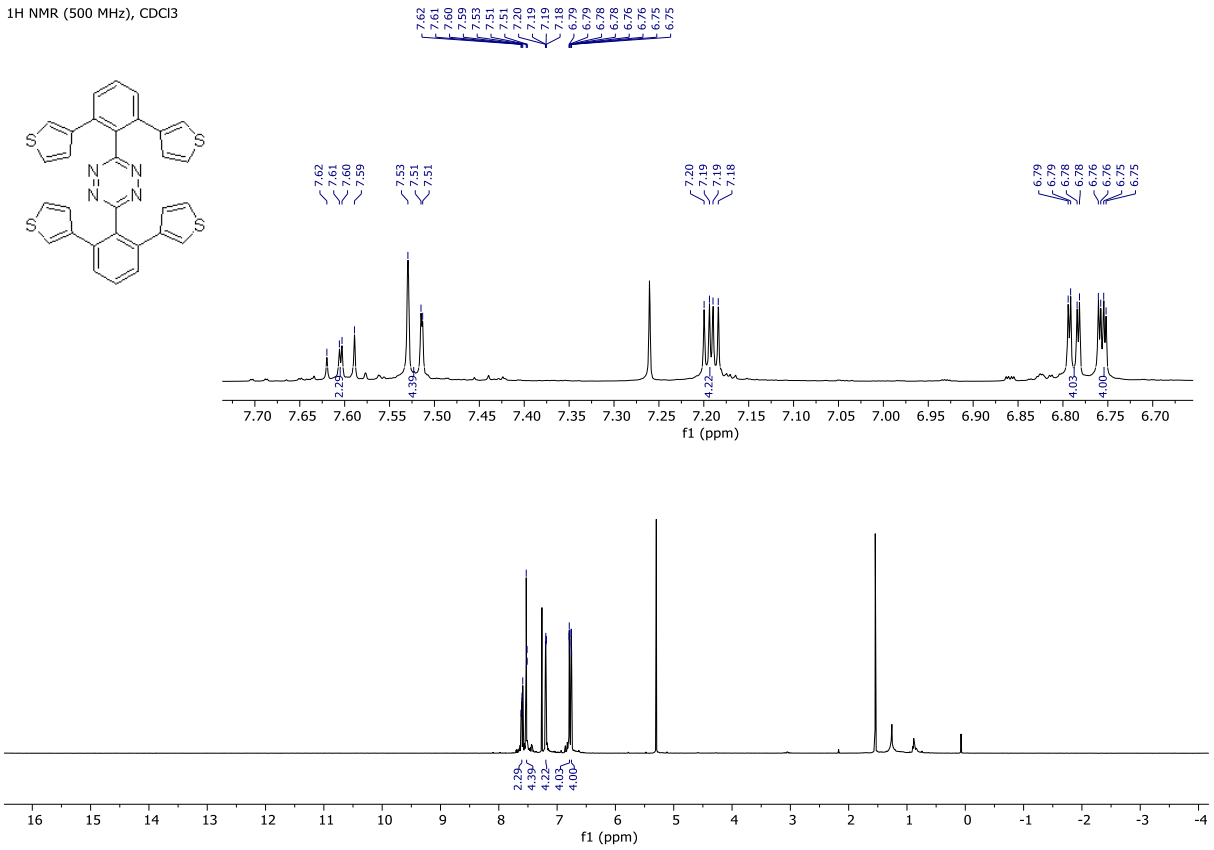

13C NMR (125 MHz), CDCl3